A novel phylogenomics pipeline reveals complex pattern of reticulate evolution in Cucurbitales

Edgardo M. Ortiz[1,2*], Alina Höwener[1], Gentaro Shigita[1,3], Mustafa Raza[1], Olivier Maurin[4,5], Alexandre Zuntini[5], Félix Forest[5], William J. Baker[5,6] & Hanno Schaefer[1]

[1] Plant Biodiversity, Department Life Science Systems, Technical University of Munich (TUM), Emil-Ramann-Str. 2, D-85354 Freising, Germany

[2] current address: Florida Museum of Natural History, University of Florida, Gainesville, FL 32611, USA

[3] Faculty of Life and Environmental Sciences, University of Tsukuba, 305-8572 Tsukuba, Japan

[4] Botanic Garden Meise, Nieuwedaan38, B-1860 Meise, Belgium

[5] Royal Botanic Gardens, Kew, Richmond, Surrey, TW9 3AE, United Kingdom

[6] Department of Biology, Aarhus University, Aarhus, Denmark

[*] E-mail: e.ortiz.v@gmail.com

Abstract.--- A diverse range of high-throughput sequencing data, such as target capture, RNA-Seq, genome skimming, and high-depth whole genome sequencing, are used for phylogenomic analyses but the integration of such mixed data types into a single phylogenomic dataset requires a number of bioinformatic tools and significant computational resources. Here, we present a novel pipeline, CAPTUS, to analyze mixed data in a fast and efficient way. CAPTUS assembles these data types, allows searching of the assemblies for loci of interest, and finally produces alignments filtered for paralogs. If reference target loci are not available for the studied taxon, CAPTUS can also be used to discover new putative homologs via sequence clustering. Compared to other software, CAPTUS allows the recovery

of a greater number of more complete loci across a larger number of species. We apply CAPTUS to assemble a comprehensive mixed dataset, comprising the four types of sequencing data for the angiosperm order Cucurbitales, a clade of about 3,100 species in eight mainly tropical plant families, including begonias (Begoniaceae) and gourds (Cucurbitaceae). Our phylogenomic results support the currently accepted circumscription of Cucurbitales except for the position of the holoparasitic Apodanthaceae, which group with Rafflesiaceae in Malpighiales. A subset of mitochondrial gene regions supports the earlier position of Apodanthaceae in Cucurbitales. However, the nuclear regions and majority of mitochondrial regions place Apodanthaceae in Malpighiales. Within Cucurbitaceae, we confirm the monophyly of all currently accepted tribes but also reveal deep reticulation patterns both in Cucurbitales and within Cucurbitaceae. We show that contradicting results among earlier phylogenetic studies in Cucurbitales can be reconciled when accounting for gene tree conflict and demonstrate the efficiency of CAPTUS for complex datasets.

Keywords.--- Angiosperms353, Cucurbitaceae, Cucurbitales, gene tree discordance, paralog filtering, genome skimming, phylotranscriptomics, nitrogen-fixing clade

Modern sequencing technology allows the rapid accumulation of large amounts of genomic data at low cost. The analysis of these raw data, however, can still be a bottleneck. Researchers who cannot afford to pay for a bioinformatics expert rely on user-friendly analysis pipelines that are accessible without specialist training. As a consequence, these pipelines are of enormous importance for the field of phylogenomics. Among them, we find PHYLUCE (Faircloth 2016) and UCEasy (Ribeiro et al. 2021) specialized in the analysis of Ultra Conserved Elements (UCEs), HYBPIPER (Johnson et al. 2016) and SECAPR (Andermann et al. 2018) aimed at target capture data, PhyloHerb (Cai et al. 2022) for genome skimming data, and more generalist pipelines, such as PhyloTol (Cerón-Romero et al. 2019),

that analyzes previously assembled transcriptomes or annotated genomes and attempts to find all the possible gene families in a taxonomic group.

HYBPIPER and SECAPR are the most commonly used pipelines for target capture data in plant phylogenomics, however, they are designed to process one sample at a time, only making use of multiple computer cores at certain stages [e.g., when assembling sequences *de novo* with SPADES (Bankevich et al. 2012)]. To process multiple samples simultaneously, the users must rely on external tools such as GNU PARALLEL (Tange 2021) or additional containerization tools (Jackson et al. 2023). This lack of native parallelization capabilities can lead to suboptimal utilization of the computing resources in high-performance clusters or workstations and reduce accessibility for non-experts, potentially causing repeatability issues due to command inconsistencies across samples or human error. Also, since these pipelines were optimized for target capture data, their processing times for other data types can be exceptionally long. In contrast, most specialized user-friendly analysis pipelines designed for restriction site associated DNA (RAD) data, are aimed to efficiently process many samples in parallel, e.g., IPYRAD (Eaton and Overcast 2020), DDOCENT (Puritz et al. 2014), and to a lesser extent, Stacks (Rochette et al. 2019). For example, IPYRAD (Eaton and Overcast 2020) uses a single or just a few consistent commands, that, combined with relatively short processing times, allow for rapid testing of alternative settings. IPYRAD allows users to summarize results of each processing step so that they can decide on the most appropriate settings needed for following steps.

With these features in mind, we developed CAPTUS, a pipeline written entirely in Python and aimed at building phylogenomic datasets from multiple types of high-throughput sequencing data (target capture, RNA-Seq, genome skimming, and high-depth whole genome sequencing). CAPTUS makes extensive use of Python's native parallel computing to process many samples simultaneously in a consistent manner. This parallelization can be automated or configured manually according to user needs. Each step has a simple basic command

79 syntax (although it can be customized with many options), provides extensive reports in
80 HTML to guide the choice of settings of the next step, and is fully logged for repeatability.
81 CAPTUS is able to extract nuclear, mitochondrial, and plastid proteins considering the different
82 genetic codes and gene characteristics of each genomic compartment, as well as any other
83 type of DNA targets (such as ribosomal RNA, introns, intergenic spacers, etc.) in a single
84 command. In HYBPIPER, this would require as many runs as target types; moreover, SECAPR
85 is not able to perform translated searches on the assemblies, limiting its targets to nucleotide
86 sequences only. During the alignment stage, CAPTUS can also filter paralogs by taking
87 advantage of reference target files that contain multiple sequences per locus such as the
88 Angiosperms353 target file, a set of genes targeted by a universal probe set (Johnson et al.
89 2019), and its more taxonomically comprehensive version Mega353 (McLay et al. 2021). The
90 final outputs of CAPTUS are multiple sequence alignments (MSAs) for each reference locus
91 found in the samples. The MSAs are organized by genomic compartment and format (amino
92 acid, nucleotide, etc.), and multiple versions of each are provided (i.e., unfiltered, paralog-
93 filtered, untrimmed, and trimmed) so the user can select which type of alignment to use for
94 phylogenetic inference. Additionally, a special feature of CAPTUS is the search for novel
95 conserved markers by clustering contigs that received no hits from the reference target loci
96 across samples, thus making use of data that otherwise would be ignored.

97 We demonstrate the potential of CAPTUS with the example of the flowering plant order
98 Cucurbitales, according to APG IV (The Angiosperm Phylogeny Group 2016) a clade of eight
99 plant families with diversity centers in the Tropics: Anisophylleaceae, Apodanthaceae,
100 Begoniaceae, Coriariaceae, Corynocarpaceae, Cucurbitaceae, Datiscaceae, and
101 Tetramelaceae. Together, they include 110 genera with more than 3,100 species, about 2,000
102 of them in the mega-diverse genus *Begonia* in Begoniaceae (Goodall-Copestake et al. 2009)
103 and 1,000 in Cucurbitaceae (Stevens 2001; Schaefer 2020). The genus *Begonia* is of great
104 horticultural importance while Cucurbitaceae include some of the most important vegetable

105 and fruit crops worldwide, like cucumber and watermelon (Schaefer and Renner 2011a).
106 Morphologically, the taxa of Cucurbitales are rather diverse, ranging from endophytic
107 holoparasites in Apodanthaceae (Bellot and Renner 2014) to annual and perennial herbs in
108 Datiscaceae and Begoniaceae, to trees and shrubs in Anisophylleaceae, Corynocarpaceae,
109 Coriariaceae, and Tetramelaceae, and finally to woody or herbaceous climbers and creepers in
110 Cucurbitaceae (Schaefer and Renner 2011a; Schaefer 2020).

111 A number of studies addressed phylogenetic problems in Cucurbitales in the past three
112 decades. The earliest comprehensive seed plant phylogeny based on *rbc*L sequences (Chase et
113 al. 1993) already identified a clade uniting the genera *Coriaria* (Coriariaceae), *Datisca*
114 (Datiscaceae), *Luffa* (Cucurbitaceae), *Cucurbita* (Cucurbitaceae), *Begonia* (Begoniaceae), and
115 *Tetrameles* (Tetramelaceae). Zhang et al. (2006) produced the first phylogeny estimate
116 focused on Cucurbitales based on nine plastid, nuclear and mitochondrial loci and confirmed
117 the results of Chase et al. (1993) while adding Anisophylleaceae and Corynocarpaceae to the
118 Cucurbitales clade. The work of Barkmann et al. (2007) suggested another surprising addition
119 to the Cucurbitales clade: based on mitochondrial *mat*R sequence data, the holoparasitic
120 Apodanthaceae were placed in Cucurbitales. Filipowicz and Renner (2010) increased the
121 *mat*R dataset of Barkmann et al. (2007), added a nuclear 18S dataset, and confirmed that the
122 holoparasitic Apodanthaceae were best placed in Cucurbitales as sister lineage to all other
123 families. Schaefer and Renner (2011b) inferred phylogenetic relationships in the order based
124 on 14 DNA regions from all three genomes, confirming the position of Apodanthaceae based
125 on *mat*R, while their nuclear 18S-ITS-26S dataset placed Apodanthaceae outside of
126 Cucurbitales. Other studies targeted individual families: Zhang et al. (2007) provided the first
127 comprehensive phylogeny estimate for Anisophylleaceae, Kocyan et al. (2007) and Schaefer
128 et al. (2009) for Cucurbitaceae, Goodall-Copestake et al. (2009) for Begoniaceae, and Renner
129 et al. (2020) for Coriariaceae. In recent years, several phylogenomic studies contributed to an
130 even better understanding of the evolutionary relationships within the family Cucurbitaceae.

Bellot et al. (2020) analyzed entire plastomes plus a set of 57 single-copy nuclear genes and the ITS region for 29 species from all but one of the accepted tribes and detected four nodes with conflicting phylogenetic signals. With an impressive set of 136 transcriptomes and full genomes of Cucurbitaceae, representing c. 50% of the genera, Guo et al. (2020) produced a well-supported phylogeny estimate for the family that conflicted with earlier studies in several positions (Kocyan et al. 2007; Schaefer et al. 2009; Schaefer and Renner 2011b). Finally, our recent angiosperm-wide analysis (Zuntini et al. 2024) in the framework of the Plant and Fungal Trees of Life (PAFTOL) project (Baker et al. 2022) with an almost complete representation of Cucurbitales at the genus level placed the holoparasitic Apodanthaceae outside Cucurbitales in Malpighiales and found a sister relationship between Cucurbitales and Rosales, challenging the results of most earlier studies.

In this study, we provide a detailed description of our new analysis pipeline CAPTUS and demonstrate how it can be used not only to extract the Angiosperms353 genes (Johnson et al. 2019), but also to derive a new set of thousands of nuclear genes from transcriptomic data and to extract all mitochondrial genes and entire plastomes for the Cucurbitales. The resulting phylogenomic datasets were analyzed with coalescent and concatenation methods to infer a complete genus-level nuclear phylogeny as well as plastid and mitochondrial phylogenies and test the earlier results for the topology of the order. We compare the performance and efficiency of CAPTUS against the most widely used pipeline in plant phylogenomics, HYBPIPER, which is also able to use amino acid sequences as reference targets and can handle multiple reference target sequences per locus.

MATERIALS & METHODS

Sampling

We used a total of 125 Cucurbitales samples. Of these, 113 are target capture sequencing samples produced for this study, but have been published previously in broader

157 angiosperm phylogenetic analyses (Baker et al. 2022; Zuntini et al. 2024), while five target
158 capture samples and seven high-depth whole genome sequencing samples have not been
159 previously published (Table S1). Additionally, we downloaded sequence data for 327 samples
160 (Cucurbitales and outgroups) available in NCBI's SRA: 240 RNA-Seq samples, 48 genome
161 skimming samples (<30x), 31 high-depth whole genome sequencing samples (>30x), and
162 eight additional target capture samples (Table S2). The entire dataset comprises 342 samples
163 of Cucurbitales sensu APG IV, representing all 110 currently accepted genera and 249 of the
164 c. 3,100 species. To test the results of our recent angiosperm-wide analysis (Zuntini et al.
165 2024) and the study of Alzate et al. (2024), who found Apodanthaceae outside Cucurbitales as
166 sister of Malpighiales or nested in Malpighiales, we selected a taxonomically broad outgroup
167 that includes 110 samples covering taxa across the three other orders of the nitrogen-fixing
168 clade (25 species in eight families of Rosales, 11 species in six families of Fagales, and 28
169 species in three families of Fabales), as well as 31 species in 23 families of Malpighiales, six
170 species in six families of Malvales, three species of Huaceae (Huales), and three species of
171 Vitaceae (Vitales).
172

173 *DNA Extraction and Sample Preparation*

174 DNA samples were taken from the DNA banks of the Plant Biodiversity group at the
175 Technical University of Munich and the Royal Botanic Gardens, Kew. Tissue samples for
176 DNA extractions came from the herbaria of the Royal Botanic Gardens, Kew (K), Muséum
177 National d'Histoire Naturelle in Paris (P), Botanische Staatssammlung München (M), and the
178 Technical University of Munich (TUM).

179 Several different methods were used for DNA extraction from herbarium material
180 intended for target capture: (i) a CTAB-chloroform-based (Doyle and Doyle 1987) protocol
181 with ethanol washes and a cesium chloride/ethidium bromide density gradient cleaning and
182 dialysis, (ii) a modified CTAB protocol (Doyle and Doyle 1987) followed by an Agencourt

183 AMPure XP bead clean-up (Beckman Coulter, Indianapolis, Indiana, USA), (iii) an SDS-
184 based protocol using Magen HiPure SF Plant DNA Kit (Angen Biotech Co., Ltd, Guangzhou,
185 China) using magnetic beads for extraction and cleaning, and (iv) the manufacturers protocol
186 of the CTAB-based NucleoSpin Plant II Extraction Kit (MACHEREY-NAGEL GmbH & Co.
187 KG, Düren, Germany) using silica columns for binding the DNA. Depending on the available
188 herbarium material, we used 20-160 mg of dry material for extraction.

189 To measure DNA quality, we evaluated fragment size distribution using an Agilent
190 Technologies 4200 TapeStation System with Genomic DNA ScreenTapes (Agilent
191 Technologies, Santa Clara, California, USA) or by electrophoresis in 1% agarose gel. DNA
192 was quantified using a Quantus™ Fluorometer (Promega Corporation, Madison, WI, USA) or
193 with a Qubit 3.0 Fluorometer (Invitrogen, Walthan, Massachusetts, USA).

194 The seven samples intended for high-depth whole genome sequencing were extracted
195 with one of the following methods: (i) the standard protocol of the CTAB-based NucleoSpin
196 Plant II Extraction Kit (MACHEREY-NAGEL GmbH & Co. KG, Düren, Germany), and (ii)
197 the standard protocol of the MagBind® Plant DNA plus 96 Kit (Omega Bio-tek Inc.
198 Norcross, Georgia, USA). These seven DNA extractions were sent to GENEWIZ Germany
199 GmbH (Leipzig, Germany), where libraries were prepared with the NEBNext Ultra II Library
200 Prep Kit for Illumina (New England BioLabs, Ipswich, Massachusetts, USA) and sequenced
201 on a NovaSeq 6000 platform (Illumina, San Diego, California, USA) with a paired-end 2x150
202 configuration.

203

204 *Library Preparation, Pooling, Target Enrichment, and Sequencing*

205 Shearing was only performed for samples with fragment sizes above 350 bp using a
206 Covaris M220 Focused-ultrasonicator with Covaris microTUBES AFA Fiber Pre-Slit Snap-
207 Cap (Covaris, Woburn, Massachusetts, USA). Libraries were prepared with the DNA
208 NEBNext UltraTM II Library Prep Kit, including size selection of DNA fragments with a

length of 300 to 400 bp using SPRI beads (Agencourt AMPure XP Bead Clean-up; Beckman Coulter, Indianapolis, IN, USA.

Libraries were grouped and pooled by similar DNA quality and quantity. For target enrichment via hybridization of the pooled libraries, we used the Arbor Biosciences myBaits Target Capture Kit, "Angiosperms353 v1" (Catalog #3081XX), following the manufacturer's manual Version 4.01 (myBaits® Kit Manual – Arbor Biosciences 2020). Hybridized libraries were PCR-amplified using the NEBNext Ultra II Q5 Master Mix (New England BioLabs, Ipswich, Massachusetts, USA). Quality and quantity of the library pools were evaluated with TapeStation and Qubit respectively as above, and then normalized and pooled for sequencing of paired-end 2x300 reads on a MiSeq platform (Illumina, San Diego, California, USA) at the Jodrell Laboratory, Royal Botanic Gardens, Kew or paired-end 2x150 reads at Macrogen Europe B.V. in Amsterdam (Macrogen, Inc., Seoul, Korea) with a HiSeq system (Illumina, San Diego, California, USA).

Sequence Analysis Workflow

CAPTUS, implemented in Python 3, is freely available and maintained through GitHub (https://github.com/edgardomortiz/Captus) including a full documentation (https://edgardomortiz.github.io/captus.docs/). It can be installed directly from Bioconda (https://bioconda.github.io/recipes/captus/README.html). The workflow of CAPTUS consists of four steps controlled by their respective modules called `clean`, `assemble`, `extract`, and `align`, which are typically run in that order (Fig. 1).

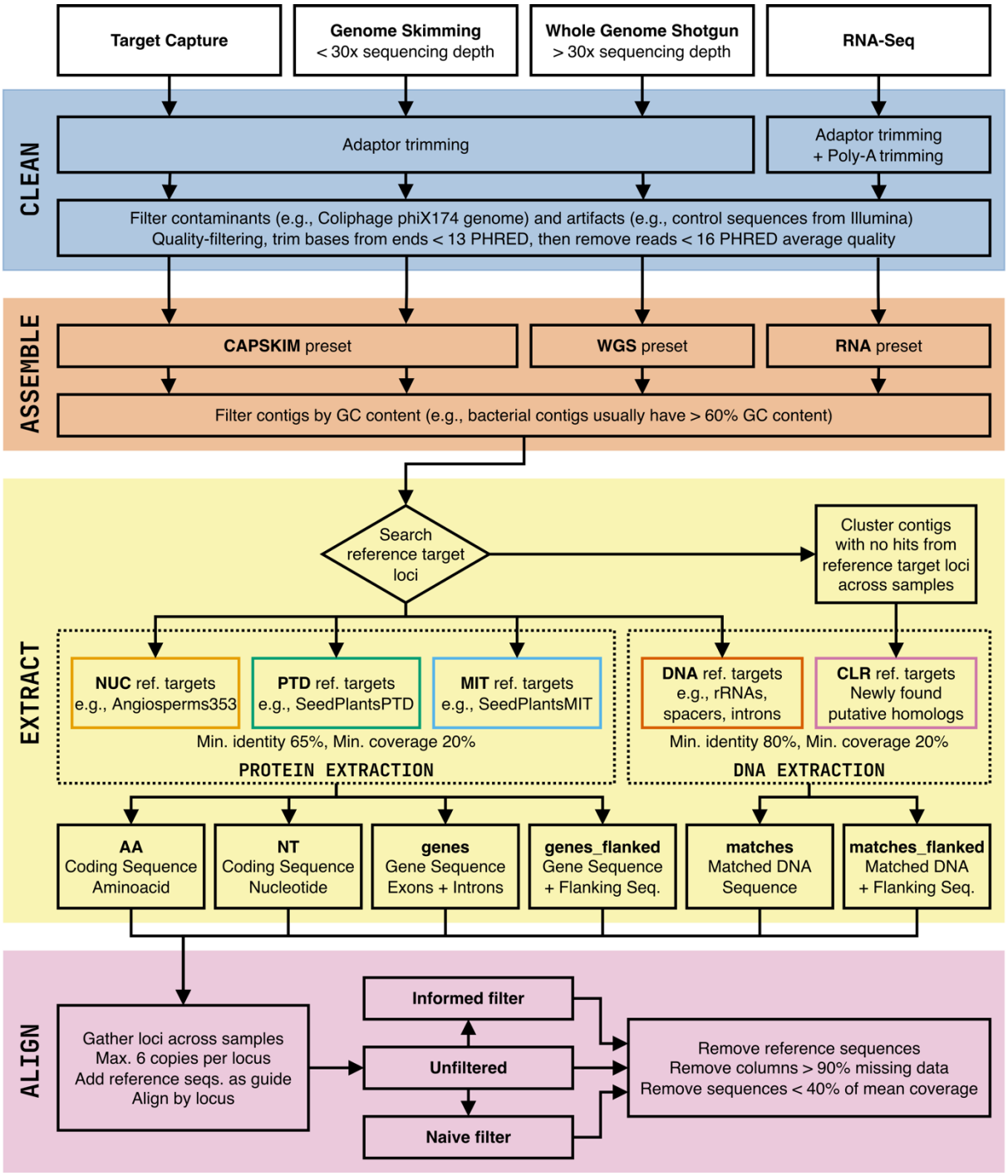

FIGURE 1. Workflow of the analysis pipeline CAPTUS. The default thresholds shown can be changed by the user via command options. NUC: nuclear proteins, PTD: plastidial proteins, MIT: mitochondrial proteins, DNA: miscellaneous DNA targets, CLR: DNA targets found via clustering

237 Alternatively, the analysis can be started at different points depending on the sample
238 data provided. If raw reads are provided one should start with the `clean` module, if the reads
239 have already been cleaned, they can be directly analyzed with the `assemble` module, and if
240 previously assembled data or reference genomes are provided the analysis can start using the
241 `extract` module. CAPTUS provides flexibility in combining samples that enter the workflow
242 at different stages. For example, a phylogenomic dataset could be composed of samples
243 represented by target capture raw sequencing reads, samples with clean RNA-Seq reads, and
244 genomic assemblies downloaded from GenBank in order to increase taxon sampling.
245
246 *The* `clean` *module.*--- CAPTUS uses BBDUK from BBTOOLS (Bushnell 2022) to clean raw
247 reads. Cleaning is performed in two steps. First, adaptors and poly-A tails (when cleaning
248 RNA-Seq reads) are trimmed in two consecutive rounds. Then, adaptor-free reads are quality-
249 trimmed, and reads matching the phiX viral genome or known sequencing artifacts are
250 removed using the databases provided by BBDUK. In this step, leading and trailing bases with
251 PHRED scores <13 are trimmed and then trimmed reads with average PHRED score <16 are
252 removed, both thresholds can be altered by the user.
253 When cleaning is completed, FASTQC (Andrews 2019) or its faster implementation
254 FALCO (de Sena Brandine and Smith 2021) is run both on the raw and the cleaned reads to
255 evaluate and compile quality statistics. Finally, CAPTUS summarizes the cleaning statistics of
256 all the samples before and after cleaning in a single HTML report that allows a quick
257 overview of all quality measurements.
258 For the Cucurbitales analysis, default settings were used for all samples in the `clean`
259 module except RNA-Seq data, for which the option `--rna` was added to trim poly-A tails.
260
261 *The* `assemble` *module.*--- The clean reads are passed to the assembly module which uses
262 MEGAHIT for *de novo* assembly. This assembler is capable of handling very large datasets in

263 a time-efficient manner and with greatly reduced memory requirements because of the use of
264 a compressed representation of *de Bruijn* graphs and very efficient parallel computing
265 algorithms. Additionally, MEGAHIT implements the concept of *mercy-kmers*, a unique
266 strategy that allows removing spurious low-depth contigs while keeping authentic ones (Li et
267 al. 2015, 2016). More importantly, the ability of assembling all reads simultaneously has been
268 found to reduce the amount of chimeric contigs (García-López et al. 2015).Thanks to these
269 features, MEGAHIT is not only exceptional at assembling metagenomic datasets (its original
270 purpose) but also single-genome datasets, and is able to produce accurate assemblies even at
271 low sequencing depths as shown in our previous tests with small datasets (Raza et al. 2023).
272 We tested several combinations of MEGAHIT settings in order to optimize the
273 assembly of other types of data. These are provided in CAPTUS under three presets: (i)
274 `CAPSKIM` for target sequence capture, genome skimming data, or a combination of both, (ii)
275 `RNA` for RNA-Seq data, and (iii) `WGS` for high-depth whole genome sequencing data, which
276 includes the recently defined "Deep genome skimming" (Liu et al. 2021)
277 (https://edgardomortiz.github.io/captus.docs/assembly/assemble/options/#--preset).
278 The `assemble` module also provides an option to subsample a fixed number of reads per
279 sample prior to assembly, which is useful when the sequencing depth is too high for a
280 particular sample or for speeding up assembly during trial runs.
281 Once assembly is completed, CAPTUS can also filter contigs based on their GC
282 content. For example, a maximum of 60% GC would be appropriate to remove bacterial
283 contamination in most eukaryotic genomes (Fierst and Murdock 2017). Finally, CAPTUS
284 computes assembly statistics and produces a single HTML report for all processed samples.
285 Target capture and genome skimming samples of the Cucurbitales were run with the
286 default assembly preset (`--preset CAPSKIM`), RNA-Seq samples were assembled using –
287 `-preset RNA`, and high-depth whole genome sequencing samples using `--preset WGS`.

288 To remove potential bacterial contamination, we used the option `--max_contig_gc 60`
289 for all assemblies.
290
291 *The `extract` module.*--- Once assemblies are completed, they can be searched for particular
292 loci of interest (i.e., reference target loci). CAPTUS allows the simultaneous search and
293 extraction of five types of markers (i) nuclear proteins (`NUC`), (ii) plastid proteins (`PTD`), (iii)
294 mitochondrial proteins (`MIT`), (iv) miscellaneous DNA regions (`DNA`), and (v) new
295 clustering-derived putative homologs (`CLR`).
296 Protein extractions (`NUC`, `PTD`, and `MIT` markers) use reference target loci provided as
297 amino acid sequences or coding sequences in nucleotides (CDS) and a different genetic code
298 can be specified for each separately. CAPTUS uses the program SCIPIO to perform protein
299 extractions. SCIPIO is able to automatically correct frameshifts that could result from
300 sequencing or assembly error and it can recover proteins and their putative paralogs that are
301 spread across several contigs by analyzing splice patterns, checking for compatible exonic
302 boundaries and overlaps, and for consistency in the similarity of the partial hits to the target
303 protein to reconstruct coherent gene models (Keller et al. 2008; Hatje et al. 2011). This is
304 important, given that loci assemblies resulting from target capture data can potentially be
305 highly fragmented, particularly when the captured target proteins contain exons that are
306 separated by long introns. CAPTUS comes bundled with four reference target sets, two `NUC`
307 references [curated versions of the Angiosperms353 (Johnson et al. 2019) target file and the
308 taxonomically expanded Mega353 (McLay et al. 2021) target file], as well as a plastid `PTD`
309 reference (SeedPlantsPTD), and a mitochondrial `MIT` reference (SeedPlantsMIT).
310 Our curation of the Angiosperms353 reference target file consisted in clustering the
311 sequences at 98% identity to remove highly similar sequences and duplicates while the
312 curation of the Mega353 reference target file consisted in removing contaminated sequences
313 (e.g., fungal, algal, organellar sequences) and then clustering at 78% identity to reduce

sequence redundancy. Thus, CAPTUS still takes advantage of the expanded taxonomic representation of the Mega353 reference targets (McLay et al. 2021) while bypassing the additional step of filtering by taxon suggested in the instructions (https://github.com/chrisjackson-pellicle/NewTargets). The `PTD` and `MIT` target references represent carefully curated sets of 83 proteins (represented by 2,194 sequences) and 45 proteins (represented by 167 sequences) respectively, found in most organellar genomes of seed plants originally downloaded from GenBank. CAPTUS also allows the utilization of BUSCO lineage databases (e.g. https://busco-data.ezlab.org/v5/data/lineages/) as target references and new target sets for organism groups other than seed plants are possible and being developed.

Miscellaneous DNA regions (`DNA`) extractions are aimed at recovering other types of `DNA` regions (e.g., complete genes with introns, non-coding regions, ribosomal genes, individual exons, RAD markers, etc.). In this case, CAPTUS uses the program BLAT (Kent 2002) to search the assembly and the hits that are found across contigs are greedily assembled and concatenated using our own code.

When a protein or DNA target is spread among several contigs, CAPTUS concatenates the contigs to reconstruct the entire locus. This procedure is carefully done as it considers the sequence identity of each fragment to the target and their mutual overlap in order to minimize the possibility of chimeras. However, if the targets are expected to be fully contained in a single contig (e.g., when using pre-assembled genomes as input) or if chimeric contigs are of high concern, contig concatenation can be disabled with `--disable_stitching`.

Additionally, CAPTUS can be used to find new putative homologs by clustering the contigs that had no hits from the reference target loci across samples. In this case, the program MMSEQS2 (Steinegger and Söding 2018) is used, and several of its settings are available through CAPTUS. Once the sequence clusters have been found, they are filtered by the number of samples in the cluster and sequence length, and representative sequences per cluster are

selected as new reference targets to perform another extraction of the miscellaneous DNA type in CAPTUS. The output from this second round of extraction is indicated by the prefix CLR.

The user can specify the minimum sequence identity and coverage to perform the search of target loci within the assemblies. If several matches are found for a single target locus, they are ranked from most to least similar and complete as compared to the reference target sequence. Therefore, the best hit is recognized in the output files by having the suffix _00 while the rest of the copies (i.e., putative paralogs) are ranked with increasing numbers (e.g., _01, _02, etc.).

The output files from protein extractions (NUC, PTD, MIT) are provided in four possible formats (Fig. S1a): the protein sequence in amino acids (AA), the coding sequence in nucleotides or CDS (NT), the complete gene sequence including introns (genes), and the complete gene sequence flanked by a fixed number of nucleotides (genes_flanked). Similarly, the output from a miscellaneous DNA extraction and clustering-derived markers (DNA, CLR), have two possible formats (Fig. S1b): the segment of sequence that was matched to the reference (matches), and the matched segments flanked by a fixed number of nucleotides (matches_flanked).

Once extractions are finished, CAPTUS collects extraction statistics (e.g., recovered marker length, similarity to the reference sequence, number of paralogs, number of contigs used in the gene assembly, etc.) from all the processed samples and produces a single HTML report that provides a quick overview of these recovery indicators across loci and samples as an interactive heatmap. For example, the user can choose to plot identity to target, recovered percentage, number of copies detected, number of contigs used in the assembly of the locus and the mean depth of coverage of those contigs, among others.

For our Cucurbitales dataset, the minimum recovery percentage was set at 20%, the default in CAPTUS. We used the option -n Angiosperms353 to extract nuclear proteins

using the bundled Angiosperms353 reference targets and `-n Mega353` to extract nuclear proteins using our curated version of the taxonomically expanded Mega353. Additionally, organellar proteins were extracted with options `-p SeedPlantsPTD` and `-m SeedPlantsMIT`. Finally, we created a custom miscellaneous DNA reference by segmenting the Cucurbitales plastomes available in GenBank in 38 pieces ranging from ~3 kbp to ~5 kbp which we stored in a FASTA file (`Plastome38.fasta`, Appendix S1) and extracted in CAPTUS using the option `-d`.

Additionally, we created a set of 5,435 reference genes derived from publicly available transcriptomic data. We took the 240 transcriptomic assemblies from CAPTUS and removed the transcripts that had hits to organellar proteins, thereby retaining only putatively nuclear transcripts. We ran CODAN (Nachtigall et al. 2021) on the nuclear transcripts in order to find coding regions within them, searching both strands and using the `PLANTS_full` model which only emits a CDS when a complete protein, from start to stop codon, is identified within the transcript. Then we clustered the CDS across samples using the `extract` module of CAPTUS, with the following options:

```
-c --mmseqs2_method easy-cluster --cluster_mode 2 --
cl_min_identity 70 --cl_seq_id_mode 1 --cl_min_coverage 66 --
cl_rep_min_len 540 --cl_min_samples 144 --cl_max_copies 4
```

. These CAPTUS options retained 5,435 clusters that were at least 540 bp in length, grouped at least 144 transcriptomic samples (60%), and contained at most an average of four gene copies. After removing within-cluster redundant sequences, the resulting reference contained 13,492 sequences representing these 5,435 CDS clusters. This reference is called from this point onwards RNA5435 (`RNA5435.fasta`, Appendix S2). The new reference targets were used in the `extract` module of CAPTUS across all 452 samples using the option `-n`

389 `RNA5435.fasta --nuc_min_score 0.15 --nuc_min_identity 70` to match
390 the clustering identity threshold used for creating the reference.
391
392 *The* `align` *module.*--- The extraction output is then processed by the alignment module.
393 Individual markers are collected across samples and organized in separate FASTA files per
394 locus. By default, CAPTUS collects a maximum of five paralogs per sample and per marker to
395 be aligned. The reference sequences are also added to each locus file to serve as alignment
396 guides in case the sequences recovered from the samples are fragmentary. Then, the
397 alignment is performed with MAFFT (Katoh and Standley 2013) or MUSCLE5 (Edgar 2022)
398 using default settings or by selecting one of their specific algorithms. However, if protein
399 sequence in amino acid (`AA`) and their corresponding CDS in nucleotides (`NT`) are aligned in
400 the same run, CAPTUS aligns the `AA` with MAFFT and then uses the `AA` alignment as template
401 for the `NT`, thus producing a codon-aware alignment for the CDS. CAPTUS also allows the
402 user to provide the sample(s) that should be considered as outgroup, in this case the program
403 will place those samples as the first sequence(s) in the alignments in the order provided. This
404 feature (`--outgroup`) takes advantage of a common feature of many phylogenetic
405 estimation programs (e.g., IQ-TREE, RAXML, MRBAYES) which arbitrarily draw the first
406 sample in the alignment at the root of their output trees.
407 Once the FASTA files are aligned, paralogs are filtered using two alternative
408 algorithms, `naive` and `informed`. Our paralog filters are computationally efficient
409 because they are based on sequence similarity comparisons, however their results might differ
410 from more computationally expensive, phylogeny-informed methods of determining
411 orthology such as ORTHOFINDER or other pipelines (Yang and Smith 2014; Emms and Kelly
412 2019; Morales-Briones et al. 2021). Consequently, CAPTUS also provides the alignments that
413 include all the paralogs found per locus (`unfiltered`) so the user can use them as input for
414 other paralog-pruning methods.

415 In the `naive` filter, only the best hit (i.e., most similar and complete as compared to
416 reference target sequence, with suffix `_00` in output files) is kept for each sample and no
417 further filtering is performed. The `informed` filtering algorithm takes advantage of
418 reference datasets that contain multiple sequences per locus, such as the Angiosperms353
419 (Johnson et al. 2019) or Mega353 (McLay et al. 2021) target files as well as the ones
420 developed for CAPTUS (SeedPlantsPTD and SeedPlantsMIT). For example, the
421 Angiosperms353 reference target set (as well as its expansion Mega353) was derived from the
422 1KP Project data (Matasci et al. 2014; One Thousand Plant Transcriptomes Initiative 2019),
423 where each gene could potentially be present in more than 1,000 species. To build a less
424 redundant sequence collection while still covering the entire phylogenetic diversity of the
425 angiosperms, each selected locus was clustered at ~70% identity, usually selecting only one
426 representative sequence per cluster for the final reference dataset. Thanks to this feature, one
427 could expect that, when analyzing a single taxonomic group such as a family or genus, all
428 samples would have a best match to only one sequence in the reference targets collection for
429 any given locus (i.e., the closest relative present in the reference targets). However, a minority
430 of samples could have one or several loci showing an inconsistent paralog ranking with
431 respect to the majority of samples because their best hit matched better a different target
432 sequence. In these cases, CAPTUS compares all recovered paralogs with the reference
433 sequence that best matches the majority of samples and reorders the paralog ranking of the
434 minority keeping only the copy that is most similar to that reference target sequence across
435 samples. Finally, it could also happen that a sample presents a single copy for a specific locus
436 but with a sequence that is much more divergent than the average in the alignment (e.g., a
437 remote paralog found in a contaminated contig). By default, CAPTUS will remove any
438 sequence with average pairwise identity that is more than 4.0 standard deviations below the
439 mean pairwise identity of the entire alignment, the number of standard deviations can be
440 changed with the option `--tolerance` or deactivated using `--tolerance -1`.

441 Modern species tree inference methods can deal with phylogenetic conflict caused by
442 ILS or introgression, but are usually limited to the analysis of single-copy gene trees (Yan et
443 al. 2022). Fortunately, in those cases, the paralog pruning method has been shown to be of
444 little consequence to the final topology, where even a random selection produced results
445 congruent with more sophisticated methods of paralog removal suggesting that these methods
446 are quite robust in the presence of paralogy (Yan et al. 2022).

447 Moreover, recently developed coalescent methods, such as ASTRAL-PRO (Zhang et
448 al. 2020; Zhang and Mirarab 2022), are capable of directly analyzing single-copy gene trees
449 as well as trees of genes with paralogs (i.e., multi-copy genes), completely bypassing the need
450 of filtering extra gene copies. To facilitate these analyses, CAPTUS not only provides the
451 alignments with paralogs but also the file required by ASTRAL-PRO for mapping the paralog
452 names to the names of the samples for species tree calculation, this file is unique and can be
453 used with any of the alignment sets produced by CAPTUS.

454 The reference target sequences are then removed from the alignments. Finally, all the
455 produced alignments and their filtered versions are trimmed using CLIPKIT (Steenwyk et al.
456 2020), which can remove alignment columns based on criteria like informativeness or
457 proportion of missing data. By default, CAPTUS removes columns with > 90% missing data
458 and sequences with < 40% mean coverage. Alternatively, a minimum number of sites per
459 column instead of a percentage can be specified with `--min_data_per_column`. As in
460 previous modules, CAPTUS computes alignment statistics as well as sample occupancy
461 statistics from all the FASTA files along all filtering and trimming stages and produces a
462 comprehensive HTML report that can be used to determine outlier markers or samples that
463 should be removed or curated more carefully before proceeding to phylogenetic analysis.

464 For the Cucurbitales data, all extracted loci were aligned in CAPTUS using MAFFT's
465 most accurate algorithm E-INS-i (`--align_method mafft_genafpair`). For coding
466 regions we used the option `-f AA,NT` to take advantage of codon-aware alignments for

467 CDS, for Plastome38 we used `-f MA`. For trimming, we used `--`
468 `min_data_per_column 6`, to keep alignment columns with six or more sequences. For
469 the Plastome38 we also decreased the tolerance of the `informed` paralog filter to `--`
470 `tolerance 2.0`.
471
472 *Phylogenetic Analyses*
473 We chose the trimmed, codon-aligned coding sequences (format `NT`) from the
474 extractions performed with reference targets sets Angiosperms353, Mega353 and RNA5435.
475 For the reference targets set Plastome38 (the plastome segments) we selected the format
476 `matches` from the CAPTUS output. We analyzed the unfiltered alignments (i.e., including
477 paralogs) as well as the alignments resulting from the `naive` and `informed` paralog
478 filtering strategies for nuclear markers but only the alignments filtered by the `informed`
479 algorithm for the plastome.
480
481 *Gene tree estimation.*--- For each individual nuclear gene alignment we inferred a phylogeny
482 using IQ-TREE v. 2.2.2.6 (Minh et al. 2020b). During the run we used MODELFINDER
483 (Kalyaanamoorthy et al. 2017) to determine the most appropriate nucleotide substitution
484 model with `-m TEST`. Nodal support was inferred from 1,000 ultrafast bootstrap replicates
485 with option `-bb 1000` (Hoang et al. 2018). For comparison purposes, we also estimated
486 nuclear gene tree phylogenies using FASTTREE v. 2.1.11 (Price et al. 2010) with the manual
487 recommended options to increase the accuracy of the search and using the GTR substitution
488 model (`-pseudo -spr 6 -mlacc 3 -slownni -gtr`).
489
490 *Species tree estimation.*--- We estimated species trees using two methods, concatenation of
491 alignments followed by maximum likelihood estimation in IQ-TREE v. 2.2.2.6 (Minh et al.

492 2020b), and coalescent estimation by summarization of quartet frequencies in gene trees using
493 ASTRAL-PRO v. 1.15.1.3 (Zhang et al. 2020; Zhang and Mirarab 2022). For concatenation,
494 each individual locus alignment must contain a single sequence per sample (no paralogs
495 allowed), therefore we can only apply this method to the alignments that were filtered for
496 paralogs, while ASTRAL-PRO was applied to the filtered alignments as well as to the
497 alignments containing multiple copies. The concatenation analyses in IQ-TREE were run with
498 the same options as for the individual gene trees, and the loci alignments were provided as
499 separate files in a single directory with the option `-p`, so IQ-TREE can automatically
500 concatenate them into a supermatrix prior to analysis. The concatenation method was applied
501 only to the set 353 nuclear genes (extracted using Angiosperm353 or Mega353), to the
502 plastome segments (Plastome38).

503 For the ASTRAL-PRO analysis, the individual gene trees calculated by IQ-TREE or
504 FASTTREE were provided as well as the required file that maps the paralog names to their
505 corresponding sample name produced by CAPTUS (`captus-`
506 `assembly_align.astral-pro.tsv`). We also increased the number of placement and
507 subsampling rounds to 16 (`-R`), as well as the proportion of taxa subsampled (`--`
508 `proportion 0.75`) and calculated alternative quartet frequencies (`-u 3`).
509

510 *Site concordance analyses.*--- In order to measure concordance between alignment sites and
511 the species tree, we performed a concordance factor analysis for each species tree (Minh et al.
512 2020a). The analysis was done in IQ-TREE v. 2.2.2.6 by supplying the species tree (`-t`), the
513 folder containing the loci alignments (`-p`), and averaging the site concordance over 1,000
514 quartets (`--scfl 1000`).
515

516 *Phylogenetic conflict analysis of selected nodes.*--- Contentious relationships in the
517 Cucurbitales are centered around the relationships among tribes in the Cucurbitaceae as well

518 as the relationships among Cucurbitales families. In order to visualize the amount of conflict
519 at selected nodes in the species tree, we used the branch quartets frequencies analysis in
520 DISCOVISTA v. 1.0 (Sayyari et al. 2018), after annotating the species belonging to each
521 Cucurbitaceae tribe, to each of the families in Cucurbitales, and to the clades in the outgroup.
522
523 *Phylogenetic network estimation.*--- We concatenated the Angiosperms353 alignments
524 filtered by the `informed` method in CAPTUS keeping only the Cucurbitales families. This
525 concatenated alignment was used as input for SPLITSTREE v. 4.18.2 (Huson and Bryant 2006)
526 in order to estimate a phylogenetic network using the Neighbor Net algorithm on a matrix of
527 uncorrected P distances.
528
529 *Mitochondrial relationships in Cucurbitales.*--- The previous phylogenetic placement of the
530 Apodanthaceae as sister to the remaining Cucurbitales was based on the signal of a *mat*R
531 dataset (Filipowicz and Renner 2010, Schaefer and Renner 2011b). To compare our
532 contradicting nuclear phylogenomic results with a more comprehensive mitochondrial dataset,
533 we examined the phylogenetic relationships of all 39 mitochondrial genes found in
534 Cucurbitales. Since three genes are trans-spliced we segmented those in two or three parts for
535 a total of 43 mitochondrial gene regions.
536 In order to obtain a full complement of mitochondrial genes while excluding
537 potentially irrelevant distant hits we tested minimum sequence identity thresholds between
538 75% and 90% with CAPTUS, and determined that 83% was the highest identity threshold at
539 which all mitochondrial genes (including *mat*R) could still be recovered from the
540 Apodanthaceae samples. Additional mitochondrial genes (e.g., *rpl2*) were not recovered for
541 Apodanthaceae above 88% minimum sequence identity.
542 We extracted the mitochondrial regions from our entire dataset using CAPTUS with a
543 minimum sequence identity of 83%, minimum coverage of 30%, and allowing a maximum of

544 two additional copies per locus (`-d SeedPlantsMIT --dna_min_identity 83 --`
545 `dna_min_coverage 30 --max_paralogs 2`). The alignment was also performed in
546 CAPTUS using MAFFT's most thorough algorithm (`--align_method`
547 `mafft_genafpair`).
548 The trimmed unfiltered alignments were analyzed with IQ-TREE v2.3.6 (Minh et al.
549 2020b) performing standard model selection by MODELFINDER, with 1,000 ultrafast
550 bootstraps, and using a fixed seed (`-m TEST -bb 1000 -seed 142857`).
551 To distinguish between "host DNA" (due to contamination or perhaps horizontal gene
552 transfer) and "parasite DNA" in the Apodanthaceae samples, we analyzed the phylogenetic
553 affinities of the sequenced gene copies. If the different copies of all three Apodanthaceae
554 samples grouped together and each was represented by a single copy only, they were
555 considered "parasite DNA". If we recovered multiple copies per gene, those that grouped with
556 the known host plants [Fabaceae (Fabales) for *Pilostyles*; *Casearia* (Salicaceae, Malpighiales)
557 for *Apodanthes*] were considered "host DNA" sequences while extra copies grouping
558 elsewhere were considered "parasite DNA". Because the curated set of target plant
559 mitochondrial proteins in CAPTUS (`SeedPlantsMIT`) was derived exclusively from non-
560 parasite Angiosperms, most matches to "host DNA" had identities equal or above 88%.
561 Therefore, if an Apodanthaceae sample had a single gene copy but did not cluster with the
562 others, we decided based on sequence similarity: sequences above 88% identity with the
563 reference were classified as "host DNA" and below 88% as "parasite DNA". In a few
564 inconclusive cases the sequences were treated as "unclear", usually when the gene tree
565 presented very low resolution.
566
567 *Benchmarking*
568 The locus recovery efficiency of CAPTUS on different data types was evaluated against
569 HYBPIPER (Johnson et al. 2016) by extracting the Angiosperms353 loci (Johnson et al. 2019)

570 from a selection of 80 samples (20 from each data type), representing all families of
571 Cucurbitales and all tribes of Cucurbitaceae (Table S3). Since the HYBPIPER workflow does
572 not include a read cleaning step, we used reads cleaned by CAPTUS as a common input for
573 both pipelines. A protein target file downloaded from
574 https://github.com/mossmatters/Angiosperms353 was used as a reference for both pipelines.
575 CAPTUS was run for the `assemble` module with the aforementioned presets optimized for
576 each data type, followed by the `extract` module with default settings. HYBPIPER v. 2.1.2
577 was run using either BLASTX (Camacho et al. 2009) or DIAMOND (Buchfink et al. 2021),
578 hereafter HYBPIPER-BLASTX and HYBPIPER-DIAMOND respectively, with an identity
579 threshold of 65% (`--thresh 65`) to equalize with that of CAPTUS. For the genome
580 skimming samples, HYBPIPER-BLASTX and HYBPIPER-DIAMOND were run with a lower
581 coverage cutoff of 1 (`--cov_cutoff 1`), as the default cutoff of 8 was considered too
582 stringent for this data type. The locus recovery efficiency of each pipeline was evaluated
583 based on three metrics: running time, number of loci recovered, and total CDS length
584 recovered. To make the running times comparable across pipelines, all commands were run
585 on the same MacOS X system equipped with a 2.7 GHz Intel Xeon E5 processor with 24
586 threads and 64 GB RAM, allocating 6 threads per sample and processing 4 samples
587 concurrently. GNU PARALLEL v. 20230122 (Tange 2021) was used to run HYBPIPER on
588 multiple samples concurrently and to record the running time spent on each sample in a log
589 file (`--joblog`). The number of loci recovered and the total CDS length recovered were
590 calculated from the stats file generated by each pipeline (`captus-
591 assembly_extract.stats.tsv` from CAPTUS and `seq_lengths.tsv` from
592 HYBPIPER). Additionally, HYBPIPER was run for the `paralog_retriever` command with
593 default settings to retrieve the detected paralog sequences. The paralog sensitivity of each
594 pipeline was evaluated based on the average number of paralogs per recovered locus. To

ensure a fair comparison, only paralogs exceeding 75% of the reference protein length were counted, in accordance with the default threshold of HYBPIPER. The statistical significance of the differences between pipelines was assessed using the Wilcoxon rank-sum test with Bonferroni correction.

To investigate the relationship between sequencing depth and locus recovery, the clean reads from each sample were mapped back to the gene sequences (exons + introns) recovered by CAPTUS using BBMAP v. 39.06 (Bushnell 2022) with settings "`kfilter=22 subfilter=15 maxindel=80`". The average sequencing depth for each locus was then calculated using the `pileup.sh` script bundled with BBMAP.

To assess the implications of differences in locus recovery efficiency among pipelines on phylogenetic inference, we estimated coalescent species trees from the CDS recovered by each pipeline and compared their topologies and nodal supports. For CAPTUS, three sets of alignments with different paralog filtering strategies (`unfiltered`, `naive`, and `informed`) were generated using the `align` module with default settings. For HYBPIPER-BLASTX and HYBPIPER-DIAMOND, two sets of alignments were generated, one with paralogs and one without. All alignments, regardless of the pipeline, were generated using MAFFT v. 7.525 (Katoh and Standley 2013) with the automatic strategy selection mode (`--auto`) and trimmed for columns with >90% missing data using CLIPKIT v. 2.2.4 (Steenwyk et al. 2020) with the gappy mode (`-m gappy`). Coalescent species trees were estimated from each set of trimmed alignments using IQ-TREE v. 2.2.2.6 (Minh et al. 2020b) and ASTRAL-PRO v. 1.15.1.3 (Zhang et al. 2020; Zhang and Mirarab 2022) following the procedure described above, and then visualized using TOYTREE v. 2.0.5 (Eaton 2020).

RESULTS

Sequencing

From our 118 library preparations for target capture, 92 (78%) worked at the first attempt. Only eight of these successful libraries needed library concentration or increased number of PCR cycles to improve their quality prior to sequencing. For the remaining 26 libraries (22%) that had to be repeated, we used material of the same herbarium voucher for 14, while we had to select a different specimen for 12. Among the repeated libraries, only two needed library concentration or increased number of PCR cycles to improve their quality prior to sequencing. Nonetheless, once the sequencing was completed, three samples had to be discarded due to insufficient data. Two of the discarded samples corresponded to replicated libraries of *Octomeles sumatrana* for which we had a replacement within the target capture batch. Only one of them, *Bambekea racemosa*, needed to be replaced by additional high-depth whole genome sequencing, which was also performed for six additional samples (for previously missing taxa). In the end, a total of 122 samples (115 target capture and 7 high-depth whole genome sequencing) yielded enough high-quality data to be used for the analyses as determined by the number of loci recovered and their completeness (Table S4).

Read Cleaning and Assembly

The RNA-Seq data from NCBI had the largest average percentage of reads and percentage of base pairs removed with 4.7% and 9.2% respectively. The target capture data had the largest average percentage of raw reads with adaptors (14.6%) but adaptors were fully removed from all data types after cleaning (Table 1: Cleaning). Average total contig length (i.e, assembly size) after removing contigs with GC content > 60% was highest for high-depth whole genome sequencing (591.1 Mbp), followed by genome skimming (289.3 Mbp), and both target capture and RNA-Seq data with c. 44 Mbp. Among the genomic data types, the most fragmented was capture data (88.3 k contigs and N50 of 513.3 bp) while high-depth whole genome sequencing data reached the largest average N50 with 5023.7 bp. The GC content matched the expectations of the data type, being lower for genome skimming (37.5%)

646 and high-depth whole genome sequencing (34.8%), and higher for the gene-centered
647 datatypes target capture (40.8%) and RNA-Seq (42.6%) (Table 1: Assembly).
648 The average GC content of the filtered contigs ranged from 59.8% to 65.4% across data types
649 (Table 1: Assembly). The target capture data had the highest average percentage of contigs
650 removed because of exceeding the threshold of 60% GC content (4%).
651
652
653 TABLE 1. Summary statistics by data type (CAP – target capture; GSK – genome skimming;
654 WGS – high-depth whole genome sequencing; RNA – RNA-seq).

	CAP		**GSK**		**WGS**		**RNA**	
	N = 126		**N = 48**		**N = 38**		**N = 240**	
	Mean	SD	**Mean**	SD	**Mean**	SD	**Mean**	SD
Raw reads (Millions)	**4.7**	2.6	**17.3**	12.1	**113.5**	99.4	**44.1**	33.2
Raw bases (Gbp)	**0.7**	0.4	**2.5**	1.8	**15.9**	12.2	**5.9**	4.4
Cleaning								
Removed reads (%)	**2.3**	2.7	**1.3**	2.3	**2.0**	3.7	**4.7**	10.3
Removed bases (%)	**8.4**	8.9	**4.2**	6.7	**4.3**	8.7	**9.2**	13.1
Raw reads with adaptors (%)	**14.6**	22.0	**5.6**	12.6	**1.8**	6.8	**8.5**	11.3
Clean reads with adaptors (%)	**0.0**	0.0	**0.0**	0.0	**0.0**	0.0	**0.0**	0.0
Assembly								
Contigs (Thousands)	**88.3**	61.1	**489.0**	261.4	**823.7**	654.3	**62.7**	37.9
Assembly size (Mbp)	**44.4**	31.7	**289.3**	162.2	**591.1**	256.3	**44.7**	23.8
N50 (bp)	**513.3**	116.1	**923.3**	964.8	**5023.7**	4384.0	**1084.0**	289.5
GC content (%)	**40.8**	3.6	**37.5**	2.7	**34.8**	1.5	**42.6**	2.1
Filtered contigs (Thousands)	**1.3**	3.1	**6.2**	20.1	**16.2**	49.1	**1.8**	6.1
Filtered contigs (%)	**4.0**	21.0	**1.8**	7.5	**1.5**	3.6	**1.9**	3.4
Filtered contigs GC content (%)	**63.3**	1.0	**64.1**	1.9	**65.4**	2.4	**62.9**	1.0
Extraction								
Angiosperms353								
Percentage of loci recov. (%)	**87.9**	19.3	**70.9**	30.7	**98.8**	4.1	**92.6**	14.0
Total CDS length recov. (kbp)	**183.8**	57.5	**137.2**	89.0	**255.9**	28.5	**229.2**	53.3
Mega353								
Percentage of loci recov. (%)	**88.0**	19.3	**71.3**	30.6	**98.9**	3.9	**92.7**	14.0
Total CDS length recov. (kbp)	**190.2**	60.6	**145.6**	95.1	**271.3**	30.1	**241.8**	57.1
RNA5435								
Percentage of loci recov. (%)	**20.8**	14.9	**61.2**	30.5	**97.4**	8.4	**90.5**	14.8
Total CDS length recov. (kbp)	**808.6**	713.6	**3964.6**	2757.1	**8207.7**	1136.5	**6968.8**	1832.1

SeedPlantsPTD								
Percentage of loci recov. (%)	**78.6**	24.9	**94.9**	5.3	**96.3**	0.7	**76.2**	20.6
Total CDS length recov. (kbp)	**45.9**	20.8	**64.8**	6.7	**67.0**	1.2	**39.9**	16.9
SeedPlantsMIT								
Percentage of loci recov. (%)	**73.9**	26.5	**92.4**	10.9	**93.7**	3.9	**63.8**	21.9
Total CDS length recov. (kbp)	**22.0**	10.6	**31.8**	4.1	**32.2**	0.9	**18.0**	8.2
Plastome38								
Percentage of loci recov. (%)	**88.6**	25.6	**99.0**	5.3	**100.0**	0.0	**81.3**	20.6
Total length recov. (kbp)	**145.3**	63.4	**208.3**	30.6	**211.7**	7.3	**106.6**	45.5

Extraction and Alignment

Since the Angiosperms353 and the Mega353 reference targets aim to recover the same set of 353 genes, gene recovery in terms of number of loci and total CDS length was very similar for both (Table 1: Extraction). The average percentage of genes recovered across data types varied from c. 71% for genome skimming to c. 99% for high-depth whole genome sequencing data while the data type with the longest total CDS lengths is high-depth whole genome sequencing with an average of 271.3 kbp and the shortest is genome skimming with an average of 145.6 kbp. However, the Mega353 reference targets recovered at most 0.4% more loci than Angiosperms353 for genome skimming and at most 0.1% more for other data types. Similarly, the Mega353 reference targets produced total CDS lengths only c. 10 kbp longer than the Angiosperms353 reference targets on average across data types.

For the RNA5435 reference targets, target capture data had the lowest average percentage of recovered loci (20.8%, SD 14.9%) as well as the shortest average total CDS length (808.6 kbp, SD 713.6 kbp). For the rest of data types, the percentage of RNA5435 genes recovered ranges from 61.2% to 97.4% while the average total CDS length ranges from 3.96 Mbp to 8.2 Mbp. Recovery of organellar proteins was also high across data types, exceeding 73% except for mitochondrial proteins from RNA-Seq data where only 63.8% of the genes were recovered. The 38 plastome segments were successfully recovered across data types, where the minimum was 81.3% for RNA-Seq data. The total aligned ungapped length

676 across samples was similar for Angiosperms353 (Fig. S2a) and Mega353 alignments (Fig.
677 S2b) with c. 85% of samples with lengths between c. 200 kbp and c. 290 kbp and only c.
678 2.5% of samples showing less than 50 kbp aligned. As for RNA5435 (Fig. S2c) around 55%
679 of samples had total ungapped aligned lengths between 6.0 and 8.2 Mbp, while around 20%
680 of the samples had less than 1 Mbp aligned, corresponding mostly to target capture samples.
681 Based on a preliminary extraction report from CAPTUS which indicated an unusually
682 high number of copies per DNA region in *Lemurosicyos variegata* (Cucurbitaceae), we
683 concluded that this sample was contaminated with DNA from another plant family. Given the
684 evolutionary distance of the contaminant, we could decontaminate the *Lemurosicyos*
685 sequences using CAPTUS and a custom reference specific for Cucurbitaceae (Supplementary
686 Method). We also identified the Cucurbitaceae sample *Xerosicyos perrieri* as cross-
687 contaminated with *Ibervillea sonorae*, another Cucurbitaceae. In this case, decontamination
688 would have implied creating a *Xerosicyos*-specific reference, which was not possible, and
689 therefore we decided to exclude the *Xerosicyos perrieri* data from further analyses. A
690 preliminary plastome phylogeny revealed additional samples with chloroplast contamination
691 or lack of sufficient data for correct placement (Table S5).
692
693 *Phylogeny estimation*
694 Coalescent species trees estimated from the set of 353 genes (using Angiosperms353
695 or Mega353 reference targets sets) or the RNA5435 gene trees, regardless if inferred from
696 paralog-filtered or unfiltered alignments, or if estimated with FASTTREE or IQ-TREE, resulted
697 in topologies with monophyletic and well-supported families in Cucurbitales and
698 monophyletic and well-supported tribes in Cucurbitaceae (Fig. 2, Fig. S3, Appendix S3).
699 Species trees calculated with the concatenation method for nuclear genes (Appendix S3) and
700 for the plastome (Fig. S4) also show monophyletic families and Cucurbitaceae tribes. The
701 holoparasitic Apodanthaceae are sister to Rafflesiaceae in Malpighiales in all inferred nuclear

species trees (Fig. S3, Appendix S3), due to their holoparasitic life form, we could not recover reliable plastome data. For the mitochondrial gene regions obtained from the three Apodanthaceae samples, the results differ remarkably between genes and gene copies (Fig. 3, Table S6, Appendix S4). Focusing on what we classify "parasite DNA", 16 mitochondrial regions support a phylogenetic position of Apodanthaceae in Malpighiales, while six regions show a placement in Cucurbitales and the remaining regions lack a well-supported phylogenetic position. For the sequences that we classify as "host DNA", there is a strong affinity to the two host clades (28 *Apodanthes* sequences in 27 regions group with Malpighiales, 25 *Pilostyles* sequences in 20 regions group with Fabales), however, in the *Pilostyles aethiopica* data, we find five gene sequences grouping with Cucurbitales and seven of unclear affinity. This indicates that the Cucurbitales link to Apodanthaceae might be biologically meaningful and perhaps the result of an ancient host-parasite relationship that has been lost with the extinction of an ancestral lineage in the family.

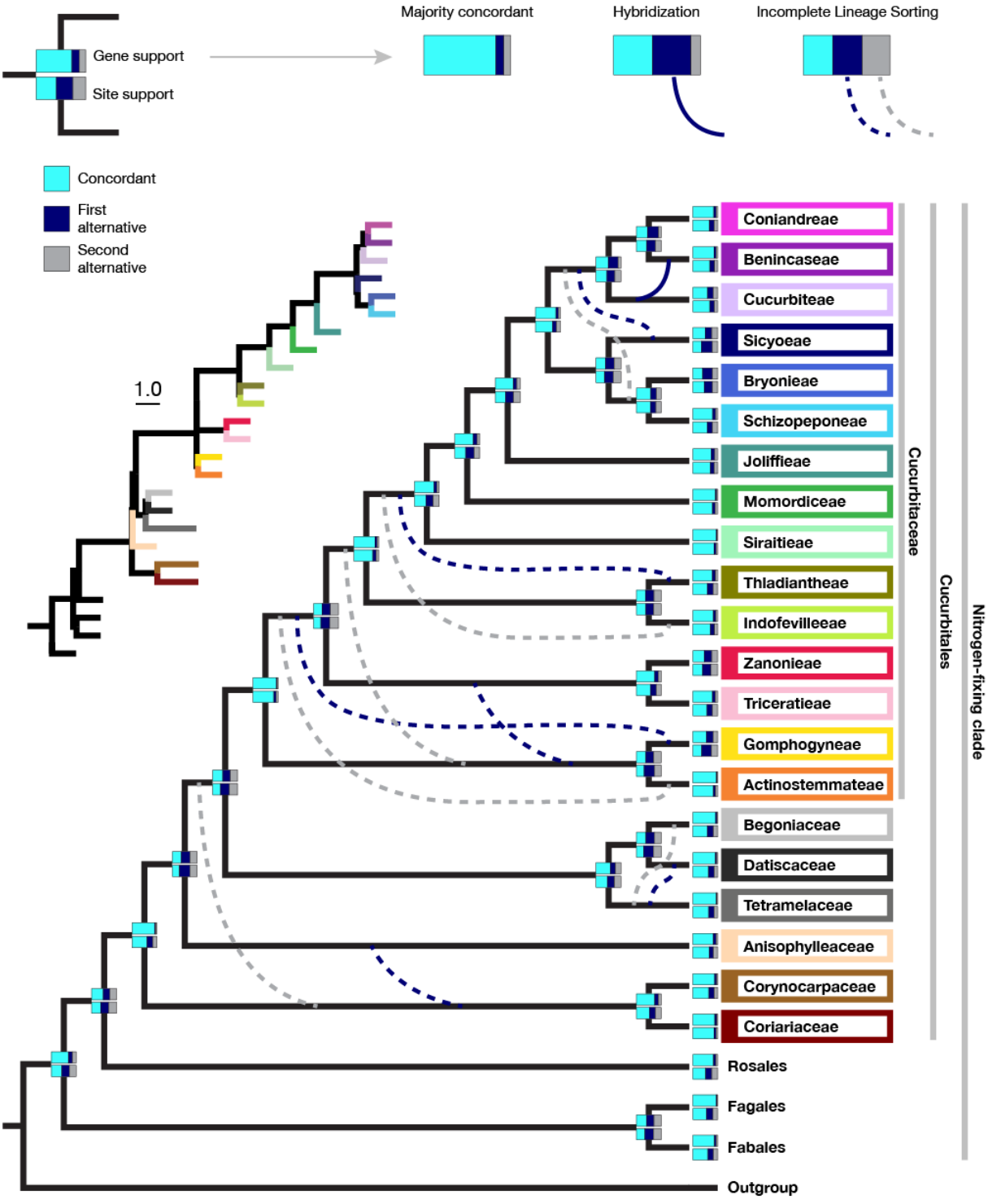

FIGURE 2. Cladogram of the Cucurbitales inferred with ASTRAL-PRO based on the RNA5435 nuclear gene trees (Fig. S5a) with families and Cucurbitaceae tribes collapsed into a single branch each. Gene support calculated with ASTRAL-PRO and site support calculated using IQ-TREE is indicated at each branch. The most frequent alternative topologies are shown with dark blue and grey broken lines for nodes under ILS and with a continuous dark blue line

722 for the node under hybridization. Internal branch lengths in the inset phylogram are in
723 coalescent units.
724

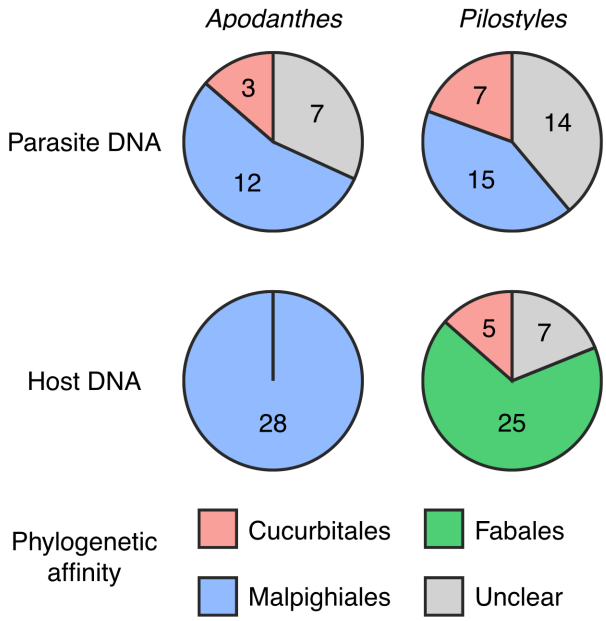

725
726 FIGURE 3. Mitochondrial affinities in the Apodanthaceae summarized by genus. The numbers
727 represent the total number of copies found in the samples.
728
729 For the remaining Cucurbitales families, the relationships vary, particularly around the
730 nodes with ambiguous quartet support surrounding short branches (see inset in Fig. 2).
731 However, the quartet frequency analyses from DISCOVISTA reveal that the apparently
732 contradicting relationships among the major clades are all compatible with the reticulations
733 depicted as dotted red lines in Fig. 2 because the different species tree configurations
734 observed coincide with the alternative quartet configurations suggested for the nodes in
735 conflict (Fig. S5). The best supported alternative shows a grade, where the clade Coriariaceae
736 + Corynocarpaceae is followed by Anisophylleaceae and by the remaining families, but there
737 is also considerable gene tree and site support for a clade in which Anisophylleaceae is sister
738 to a clade comprising Corynocarpaceae + Coriariaceae and the remainder of the order (Fig. 2).

The woody Tetramelaceae is resolved as sister to the two herbaceous families Begoniaceae and Datiscaceae but again there is also considerable gene support for the two alternative combinations within the triplet (Fig. 2). Within Cucurbitaceae, the best supported topology is a clade comprising Actinostemmateae and Gomphogyneae as sister to the remaining tribes. Among the genera with multiple samples, only *Kedrostis* is found to be polyphyletic (Fig. S3, Appendix S3, Fig. S4). The extinct Cambodian species *Khmeriosicyos harmandii*, known only from the type collection, is confidently placed in Benincaseae as sister to *Borneosicyos* from Mount Kinabalu in the nuclear species trees (Fig. S3, Appendix S3) and in a clade with *Borneosicyos* and the southeast Asian *Solena* in the plastome tree (Fig. S4). The network analysis revealed a deep reticulation within and between Benincaseae and Cucurbiteae and betweeen Schizopeponeae and Sicyoeae. There is also evidence for more recent reticulation within Coniandreae and very recent within Thladiantheae (Fig. S6). The species trees resulting from the concatenated analysis of the complete plastomes (Fig. S4) agree with the reticulated representation of the Cucurbitales topology (Fig. 2, Fig. S6).

Comparison with HYBPIPER

The locus recovery efficiency of CAPTUS with the four different data types was evaluated against the two methods offered by HYBPIPER based on running time, number of loci recovered, and total CDS length recovered (Fig. 4a). In terms of running time, HYBPIPER-DIAMOND was the fastest, followed by CAPTUS, and then HYBPIPER-BLASTX across all tested data types, except for genome skimming, where no significant difference was found between CAPTUS and HYBPIPER-BLASTX. For the number and length of loci recovered, CAPTUS consistently recovered more loci and longer sequences than both HYBPIPER-BLASTX and HYBPIPER-DIAMOND across all tested data types. The difference in locus recovery was most pronounced in the genome skimming samples, where HYBPIPER-BLASTX and HYBPIPER-DIAMOND recovered fewer than ten loci in most samples even with the lowered

coverage cutoff, while CAPTUS recovered at least 23.9 kb of CDS from 87 loci (Table S3). Across all tested data types, samples with lower sequencing depth tended to show greater differences in locus recovery between CAPTUS and HYBPIPER (Fig. S7). Additionally, the average sequencing depth of loci recovered only by CAPTUS was evidently lower than that of loci recovered also by HYBPIPER-BLASTX or HYBPIPER-DIAMOND (Fig. S8), highlighting the sensitivity of CAPTUS to samples with low sequencing depth. CAPTUS also showed higher sensitivity in paralog detection, recovering more paralogs than HYBPIPER-BLASTX and HYBPIPER-DIAMOND across all tested data types (Fig. S9). Collectively, these results demonstrate that although CAPTUS is slower than HYBPIPER-DIAMOND, it can extract more information for subsequent analyses with less bias across different data types, in a comparable or shorter time than HYBPIPER-BLASTX.

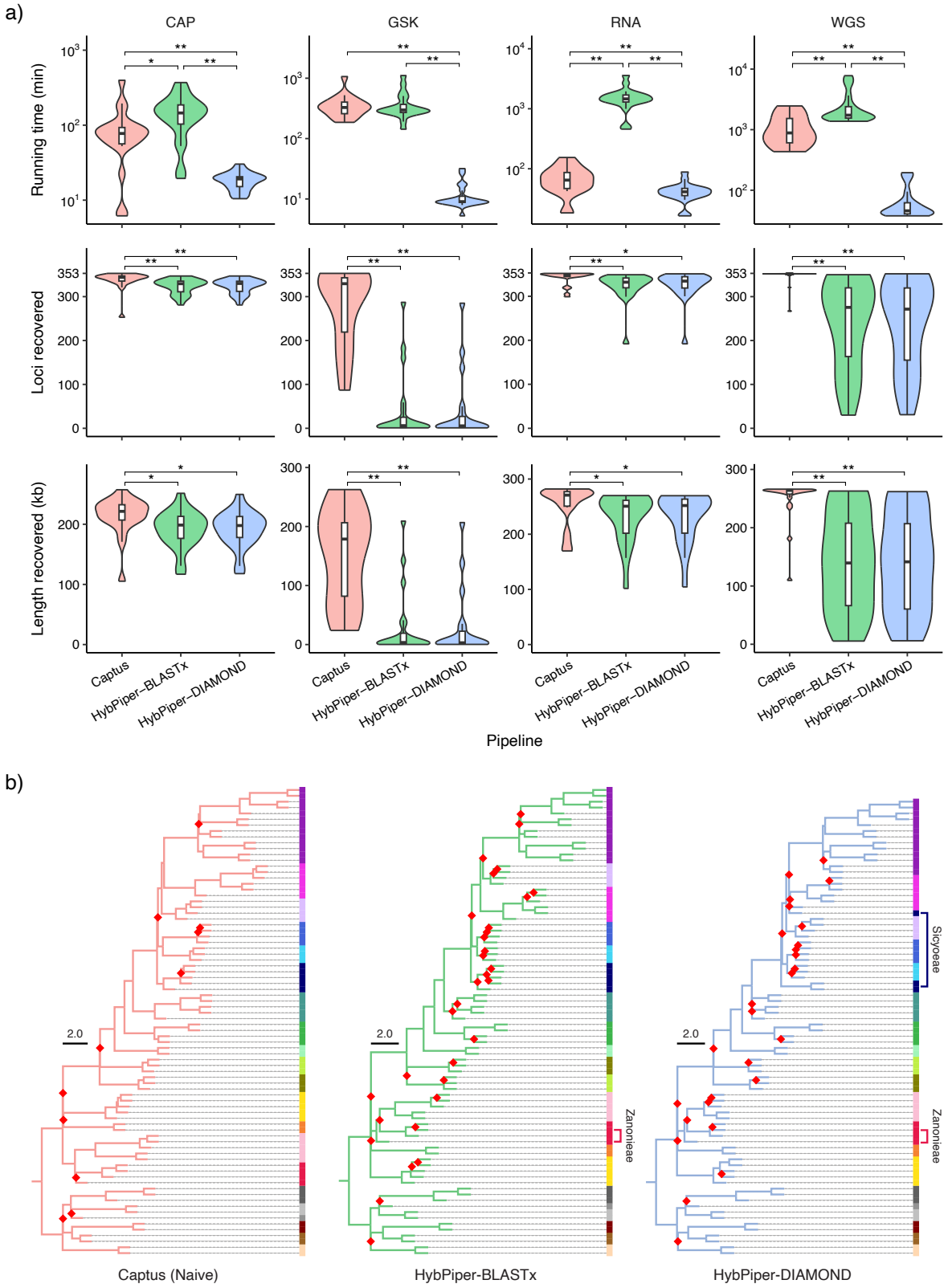

FIGURE 4. Benchmarking of CAPTUS against HYBPIPER-BLASTX and HYBPIPER-DIAMOND using a selection of 80 samples belonging to four different data types (CAP – target capture; GSK – genome skimming; RNA – RNA-seq; WGS – high-depth whole genome sequencing).

781 **a)** Comparison of locus recovery efficiency between pipelines for each data type, evaluating
782 the running time required for the assembly and extraction of the Angiosperms353 loci (top),
783 the number of loci recovered (middle), and the total length of coding sequences recovered
784 (bottom). Statistical testing was performed using the Wilcoxon rank-sum test with Bonferroni
785 correction: * $p < 0.05$, ** $p < 0.01$. **b)** Coalescent species trees estimated from CDS
786 alignments filtered for paralogs, resulting from each pipeline. Vertical bar along each tree
787 color-codes the different tribes/families in the Cucurbitales. Red diamonds indicate nodes
788 with a local posterior probability below 0.9. Tribes inferred as polyphyletic groups in the
789 HYBPIPER trees are indicated by their names and positions. Species trees resulting from the
790 alternative paralog filtering strategies are shown in Fig. S10. Trimmed alignments as well as
791 the derived tree files in NEWICK format are provided in Appendix S5.
792
793 The differences in locus recovery efficiency between the pipelines are reflected in the
794 results of phylogenetic inference (Fig. 4b, Fig. S10, Appendix S5). In the coalescent species
795 trees resulting from CAPTUS, all genera, tribes, and families were recovered as monophyletic
796 groups. In contrast, one tribe and two tribes were recovered as polyphyletic groups in the trees
797 resulting from HYBPIPER-BLASTX and HYBPIPER-DIAMOND, respectively. These
798 polyphylies are likely due to misplacement of *Sicyos edulis* (Sicyoeae) and *Siolmatra*
799 *pentaphylla* (Zanonieae), for which HYBPIPER-BLASTX and HYBPIPER-DIAMOND
800 recovered less than 40 loci, whereas CAPTUS recovered more than 250 loci (Table S3). In
801 terms of nodal support, the trees resulting from CAPTUS had fewer nodes with low support
802 (local posterior probability < 0.9) compared to those resulting from HYBPIPER-BLASTX and
803 HYBPIPER-DIAMOND. Regardless of the pipeline, the use of paralogs or alternative filtering
804 strategies did not significantly affect the species trees, except that alternative topologies were
805 adopted for some of the conflicting nodes (Fig. S10).
806

DISCUSSION

Our analysis of the mixed Cucurbitales sequence data shows that CAPTUS can handle complex datasets including low-quality and contaminated sequence data and help disentangle challenging biological phenomena like reticulation and evolution of holoparasites.

In comparison with similar existing pipelines, we find that CAPTUS is slower than HYBPIPER-DIAMOND but with our dataset recovers a higher number of more complete genes across a larger number of species than either HYBPIPER-BLASTX or HYBPIPER-DIAMOND (Fig. 4a). The obvious question arises if those additional and longer sequences recovered by CAPTUS are reliable or maybe chimeric or very low-depth sequences that could result in misleading topologies. In the case of the Cucurbitales, the tree topologies based on the CAPTUS alignments seem more reliable than the corresponding topologies from HYBPIPER. In our previous study using simulated reads at different sequencing depths, CAPTUS was shown to be capable of recovering long and accurate sequences even at low sequencing depths [Fig. 3 in (Raza et al. 2023)]. Similar to the Cucurbitales results, a higher degree of agreement among CAPTUS gene trees than for other pipelines in this earlier study [Fig. 6 in (Raza et al. 2023)] also suggests that the sequence data recovered by CAPTUS is reliable. Turning to running time, the result of this study is inconsistent with our previous finding, in which CAPTUS was the fastest among the tested pipelines, including HYBPIPER-DIAMOND [Fig. 1 in (Raza et al. 2023)]. We hypothesize that this discrepancy can be attributed to differences in the number of target loci between the two studies: this study focused on the Angiosperms353 loci, whereas Raza et al. (2023) used a custom set of 1,180 loci. The computational cost of every step in the HYBPIPER workflow, such as distributing reads to individual loci, assembling them into contigs, and matching those contigs to reference sequences, is expected to increase proportionally to the number of target loci. In contrast, in the CAPTUS workflow, the computational cost of the `clean` and `assemble` modules remains constant regardless of the number of target loci, while only the `extract` and `align` modules are affected. This

833 fundamental difference in workflow between the two pipelines may account for the
834 inconsistent running time results, warranting further investigation.

835 The strong performance of CAPTUS in locus recovery can likely be explained by a
836 combination of factors. First, the *de novo* assembly by MEGAHIT allows the assembly of *all*
837 reads in the sample in contrast to HYBPIPER which only assembles subsets of prefiltered reads
838 that match the reference loci, leading to a more restricted assembly potentially missing
839 intronic regions and small exons and decreasing assembly contiguity in general. Second,
840 SCIPIO's capacity to reconstruct gene models across several contigs is essential to recover
841 longer loci from fragmentary assemblies such as the ones resulting from target capture data
842 and particularly genome skimming (Keller et al. 2008; Hatje et al. 2011). Finally, thanks to its
843 improved reconstruction of short exons and intron splice sites as well as the ability to
844 automatically reconstruct genes across multiple contigs, SCIPIO (Keller et al. 2008; Hatje et al.
845 2011) outperforms EXONERATE (Slater and Birney 2005), the method implemented in
846 HYBPIPER.

847 The ability of CAPTUS to successfully combine different data types is confirmed by the
848 topological results where different kinds of sequence datasets for the same species,
849 consistently formed well-supported and stable clades (Supplement Trees). Also, by
850 assembling the entire set of reads in a sample, CAPTUS uses off-target reads efficiently instead
851 of excluding them a priori like HYBPIPER. Since target enrichment via DNA hybridization is
852 an imperfect process, it commonly carries over an important amount of off-target data that
853 can be useful for phylogenomics. Despite targeting only 353 genes, CAPTUS was able to find
854 almost three times as many nuclear genes (c. 1130 genes on average) using our RNA5435
855 reference targets, as well as every plastidial and mitochondrial protein and mostly complete
856 plastomes. Even though the number of off-target reads will greatly depend on hybridization
857 conditions, these are usually similar for a given set of samples and a pipeline like CAPTUS can
858 take better advantage of these other genomic regions that would remain unused otherwise.

Regarding the phylogeny estimate, our results show a well-supported nitrogen-fixing clade where Cucurbitales + Rosales are sister to Fabales + Fagales (Fig. S3, Appendix S3, Fig. S5). This topology has also been recovered by recent nuclear phylogenomic analyses (Guo et al. 2021; Zuntini et al. 2024) but differs from phylogenetic estimates mostly based on chloroplast data (Soltis et al. 1995; The Angiosperm Phylogeny Group 2016; Li et al. 2021) where the topology (Fabales (Rosales (Cucurbitales, Fagales) is recovered. Assuming the gain of nitrogen-fixing ability evolved in the common ancestor of this clade, the net number of independent losses inside the clade (e.g., Griesmann et al. 2018) should not be affected by this new topology, however future studies on the subject could benefit by also interpreting gains and losses according to this new topology. Within the Cucurbitales, all the currently accepted families are recovered as monophyletic groups in our analyses (Fig. 2, Fig. S3, Appendix S3, Fig. S4, Fig. S5). The relationships among families agree well with previous phylogenetic and phylogenomic studies of Cucurbitales, except for the position of the holoparasitic Apodanthaceae, where we find strong support for a position outside Cucurbitales, in contrast to the earlier results of Filipowicz and Renner (2010). We show that those earlier results can be explained by the phylogenetic signal coming from a subset of the mitochondrial genes (including the previously analyzed *mat*R region, which coincidentally is the most divergent gene in the mitochondria of Apodanthaceae), while *most* mitochondrial genes group with Malpighiales. This affinity of Apodanthaceae with Malpighiales is further strongly supported by the nuclear data and in agreement with our recent result based on a 58% sampling of the 13,600 genera of angiosperms (Zuntini et al. 2024). However, the results of the CAPTUS analyses indicate a highly supported sister group relationship between the Apodanthaceae and the Rafflesiaceae (Fig. S3, Appendix S3, Fig. S5) while in our previous angiosperm-wide analysis (Zuntini et al. 2024) this is not clear. The results of Alzate et al. (2024) with a reduced taxonomic sampling seem to support the inclusion of Apodanthaceae in Rafflesiaceae but a deeper phylogenomic analysis of Malpighiales that takes advantage of the increased

taxon sampling in Zuntini et al. (2024) and our increased gene sampling might be required for a robust test of these relationships.

Even though there is strong evidence of horizontal gene transfer between parasites and hosts in Angiosperms, where the parasites can act either as donors or recipients mainly via DNA-mediated transfer events, such transfers are considered "recent" and usually functional and pseudogenized copies persist in the recipient (Mower et al. 2010). The pattern observed in this study for the subset of mitochondrial genes with a close relationship between Apodanthaceae and Cucurbitales does not show any of these characteristics and therefore is a question worth investigating with a deeper analysis.

For the autotrophic families we find most support for a grade where the clade Coriariaceae + Corynocarpaceae is followed by Anisophylleaceae, a clade with the triplet Tetramelaceae plus Begoniaceae and Datiscaceae, and by Cucurbitaceae (Fig. 2, Fig. S3a, Fig. S5). Earlier studies placed Anisophylleaceae as sister to all other except Apodanthaceae (Zhang et al. 2006; Schaefer and Renner 2011b; Zuntini et al. 2024). Even though our analyses show the highest support for the clade Coriariaceae + Corynocarpaceae as sister to the remaining Cucurbitales, there is almost equal support among gene trees for Anisophylleaceae as sister to the rest (as in previous studies) as well as for a clade (Anisophylleaceae (Coriariaceae, Corynocarpaceae)) as sister to the rest of families in the order (Fig. 2, Fig. S3a, Fig. S5). For Datiscaceae, Zhang et al. (2006) and Schaefer and Renner (2011b) also found a sister group relationship to Begoniaceae, albeit with low support. Here, we find that such a clade has the highest gene tree support but the alternatives Datiscaceae sister to Tetramelaceae [recovered by Zuntini et al. (2024)] and Datiscaceae sister to Begoniaceae + Tetramelaceae also receive almost equal support (Fig. 2, Fig. S5). In the network (Fig. S6), the two dioecious families Datiscaceae + Tetramelaceae form a clade, which is sister to the monoecious Begoniaceae.

Tribal relationships within Cucurbitaceae match well the phylotranscriptomics results of Guo et al. (2020). The four conflicting nodes identified in Bellot et al. (2020) concerning the position of *Luffa*, *Hodgsonia*, *Bryonia*, and *Indofevillea* are stable when coalescent and concatenated phylogeny estimates are compared (Fig. S3, Appendix S3): *Indofevillea* is placed as sister to the Southeast Asian Thladiantheae; the sponge gourds (*Luffa*) are sister to all other Sicyoeae; the Asian *Hodgsonia* with the Neotropical Sicyoeae are sister to *Trichosanthes*; and Bryonieae plus Schizopeponeae are sister to Sicyoeae. Looking at the gene tree analyses, however, the considerable number of trees supporting alternative positions of those lineages is evident (Fig. 2, indicated in dark blue and grey dotted lines), indicating frequent hybridization events in the evolutionary history of Cucurbitaceae.

CAPTUS allows the disentanglement of the complex pattern of deep reticulated evolution in Cucurbitales, which seems to be prevalent across the angiosperms (Stull et al. 2023). The comparison of the gene tree frequencies obtained from the 353 captured regions (Angiosperms353, or the taxonomically expanded Mega353) with the frequencies obtained from the RNA5435 regions shows stable 1/3:1/3:1/3 ratio for nodes showing incomplete lineage sorting (e.g., nodes 14, 24, 29, 32, and 41 in Fig. S5a) or 1/2:1/2:0 ratio for nodes of hybrid origin (e.g., node 7 in Fig. S5a). This indicates that adding more genomic regions is unlikely to change the family and tribal level relationships in Cucurbitales found in our study. Future work should focus on the more recent evolutionary history of the clade and phylogenetic patterns within Cucurbitaceae genera.

In conclusion, we show that our new pipeline can handle a complex phylogenomic analysis in a very efficient way, maximizing the amount of recovered data in a reasonable time frame while maintaining outputs organized across a large number of samples and loci. The clustering capability of CAPTUS enables its application not only to seed plants but to any taxonomic group, even those where a reference set of orthologous loci has not yet been developed. Thus, CAPTUS can be used as a user-friendly universal tool for the assembly of

phylogenomic datasets, even with mixed data of different origins and degraded or contaminated samples.

DATA AVAILABILITY

All the original sequence data is available in Genbank (see Table S1 for accession numbers), Captus commands to reproduce the results are provided in the Material and Methods section.

ACKNOWLEDGEMENTS

We are grateful to the curators of the herbarium of Royal Botanic Gardens, Kew (K), the herbarium of Muséum National d'Histoire Naturelle in Paris (P), and the herbarium of the Botanische Staatssammlung München (M) for permission to extract DNA from selected specimens. We also thank A. Tellier (TUM) for access to the Population Genetics HPC and B. Faircloth and an anonymous reviewer for comments that help to improve the manuscript. The study was funded by the German Science Foundation DFG - SCHA 1875/4-2 within SPP 1991 Taxon-Omics (to HS), and by grants from the Calleva Foundation to the Plant and Fungal Trees of Life Project (PAFTOL) at the Royal Botanic Gardens, Kew.

REFERENCES

Alzate J.F., González F.A., Pabón-Mora N. 2024. Back together: Over 1000 single-copy nuclear loci and reproductive features support the holoendoparasitic Apodanthaceae and Rafflesiaceae as sister lineages in the order Malpighiales. Molecular Phylogenetics and Evolution. 201:108217.

Andermann T., Cano Á., Zizka A., Bacon C., Antonelli A. 2018. SECAPR—a bioinformatics pipeline for the rapid and user-friendly processing of targeted enriched Illumina sequences, from raw reads to alignments. PeerJ. 6:e5175.

Andrews S. 2019. FastQC: A quality control analysis tool for high throughput sequencing data. Available from https://github.com/s-andrews/FastQC.

Baker W.J., Bailey P., Barber V., Barker A., Bellot S., Bishop D., Botigué L.R., Brewer G., Carruthers T., Clarkson J.J., Cook J., Cowan R.S., Dodsworth S., Epitawalage N.,

Françoso E., Gallego B., Johnson M.G., Kim J.T., Leempoel K., Maurin O., Mcginnie C., Pokorny L., Roy S., Stone M., Toledo E., Wickett N.J., Zuntini A.R., Eiserhardt W.L., Kersey P.J., Leitch I.J., Forest F. 2022. A Comprehensive Phylogenomic Platform for Exploring the Angiosperm Tree of Life. Systematic Biology. 71:301–319.

Bankevich A., Nurk S., Antipov D., Gurevich A.A., Dvorkin M., Kulikov A.S., Lesin V.M., Nikolenko S.I., Pham S., Prjibelski A.D., Pyshkin A.V., Sirotkin A.V., Vyahhi N., Tesler G., Alekseyev M.A., Pevzner P.A. 2012. SPAdes: A New Genome Assembly Algorithm and Its Applications to Single-Cell Sequencing. Journal of Computational Biology. 19:455–477.

Barkman T.J., McNeal J.R., Lim S.-H., Coat G., Croom H.B., Young N.D., dePamphilis C.W. 2007. Mitochondrial DNA suggests at least 11 origins of parasitism in angiosperms and reveals genomic chimerism in parasitic plants. BMC Evol Biol. 7:248.

Bellot S., Mitchell T.C., Schaefer H. 2020. Phylogenetic informativeness analyses to clarify past diversification processes in Cucurbitaceae. Sci Rep. 10:488.

Bellot S., Renner S. 2014. The systematics of the worldwide endoparasite family Apodanthaceae (Cucurbitales), with a key, a map, and color photos of most species. PhytoKeys. 36:41–57.

Buchfink B., Reuter K., Drost H.-G. 2021. Sensitive protein alignments at tree-of-life scale using DIAMOND. Nat Methods. 18:366–368.

Bushnell B. 2022. BBTools: A suite of fast, multithreaded bioinformatics tools designed for analysis of DNA and RNA sequence data. Available from https://jgi.doe.gov/data-and-tools/software-tools/bbtools/.

Cai L., Zhang H., Davis C.C. 2022. PhyloHerb: A high‐throughput phylogenomic pipeline for processing genome skimming data. Appl Plant Sci. 10:e11475.

Camacho C., Coulouris G., Avagyan V., Ma N., Papadopoulos J., Bealer K., Madden T.L. 2009. BLAST+: architecture and applications. BMC Bioinformatics. 10:421.

Cerón-Romero M.A., Maurer-Alcalá X.X., Grattepanche J.-D., Yan Y., Fonseca M.M., Katz L.A. 2019. PhyloToL: A Taxon/Gene-Rich Phylogenomic Pipeline to Explore Genome Evolution of Diverse Eukaryotes. Molecular Biology and Evolution. 36:1831–1842.

Chase M.W., Soltis D.E., Olmstead R.G., Morgan D., Les D.H., Mishler B.D., Duvall M.R., Price R.A., Hills H.G., Qiu Y.-L., Kron K.A., Rettig J.H., Conti E., Palmer J.D., Manhart J.R., Sytsma K.J., Michaels H.J., Kress W.J., Karol K.G., Clark W.D., Hedren M., Gaut B.S., Jansen R.K., Kim K.-J., Wimpee C.F., Smith J.F., Furnier G.R., Strauss S.H., Xiang Q.-Y., Plunkett G.M., Soltis P.S., Swensen S.M., Williams S.E., Gadek P.A., Quinn C.J., Eguiarte L.E., Golenberg E., Learn G.H., Graham S.W., Barrett S.C.H., Dayanandan S., Albert V.A. 1993. Phylogenetics of Seed Plants: An Analysis of Nucleotide Sequences from the Plastid Gene rbcL. Annals of the Missouri Botanical Garden. 80:528.

Doyle J.J., Doyle J.L. 1987. A rapid DNA isolation procedure for small quantities of fresh leaf tissue. Phytochemical Bulletin. 19:11–15.

1008 Eaton D.A.R. 2020. Toytree: A minimalist tree visualization and manipulation library for
1009 Python. Methods Ecol Evol. 11:187–191.

1010 Eaton D.A.R., Overcast I. 2020. ipyrad: Interactive assembly and analysis of RADseq
1011 datasets. Bioinformatics. 36:2592–2594.

1012 Edgar R.C. 2022. Muscle5: High-accuracy alignment ensembles enable unbiased assessments
1013 of sequence homology and phylogeny. Nat Commun. 13:6968.

1014 Emms D.M., Kelly S. 2019. OrthoFinder: phylogenetic orthology inference for comparative
1015 genomics. Genome Biol. 20:238.

1016 Faircloth B.C. 2016. PHYLUCE is a software package for the analysis of conserved genomic
1017 loci. Bioinformatics. 32:786–788.

1018 Fierst J.L., Murdock D.A. 2017. Decontaminating eukaryotic genome assemblies with
1019 machine learning. BMC Bioinformatics. 18:533.

1020 Filipowicz N., Renner S.S. 2010. The worldwide holoparasitic Apodanthaceae confidently
1021 placed in the Cucurbitales by nuclear and mitochondrial gene trees. BMC Evol Biol.
1022 10:219.

1023 García-López R., Vázquez-Castellanos J.F., Moya A. 2015. Fragmentation and Coverage
1024 Variation in Viral Metagenome Assemblies, and Their Effect in Diversity
1025 Calculations. Front. Bioeng. Biotechnol. 3.

1026 Goodall-Copestake W.P., Harris D.J., Hollingsworth P.M. 2009. The origin of a mega-diverse
1027 genus: dating *Begonia* (Begoniaceae) using alternative datasets, calibrations and
1028 relaxed clock methods. Botanical Journal of the Linnean Society. 159:363–380.

1029 Griesmann M., Chang Y., Liu X., Song Y., Haberer G., Crook M.B., Billault-Penneteau B.,
1030 Lauressergues D., Keller J., Imanishi L., Roswanjaya Y.P., Kohlen W., Pujic P.,
1031 Battenberg K., Alloisio N., Liang Y., Hilhorst H., Salgado M.G., Hocher V., Gherbi
1032 H., Svistoonoff S., Doyle J.J., He S., Xu Y., Xu S., Qu J., Gao Q., Fang X., Fu Y.,
1033 Normand P., Berry A.M., Wall L.G., Ané J.-M., Pawlowski K., Xu X., Yang H.,
1034 Spannagl M., Mayer K.F.X., Wong G.K.-S., Parniske M., Delaux P.-M., Cheng S.
1035 2018. Phylogenomics reveals multiple losses of nitrogen-fixing root nodule symbiosis.
1036 Science. 361:eaat1743.

1037 Guo J., Xu W., Hu Y., Huang J., Zhao Y., Zhang L., Huang C.-H., Ma H. 2020.
1038 Phylotranscriptomics in Cucurbitaceae Reveal Multiple Whole-Genome Duplications
1039 and Key Morphological and Molecular Innovations. Molecular Plant. 13:1117–1133.

1040 Guo X., Fang D., Sahu S.K., Yang S., Guang X., Folk R., Smith S.A., Chanderbali A.S., Chen
1041 S., Liu M., Yang T., Zhang S., Liu X., Xu X., Soltis P.S., Soltis D.E., Liu H. 2021.
1042 Chloranthus genome provides insights into the early diversification of angiosperms.
1043 Nat Commun. 12:6930.

1044 Hatje K., Keller O., Hammesfahr B., Pillmann H., Waack S., Kollmar M. 2011. Cross-species
1045 protein sequence and gene structure prediction with fine-tuned Webscipio 2.0 and
1046 Scipio. BMC Res Notes. 4:265.

1047 Hoang D.T., Chernomor O., von Haeseler A., Minh B.Q., Vinh L.S. 2018. UFBoot2:
1048 Improving the Ultrafast Bootstrap Approximation. Molecular Biology and Evolution.
1049 35:518–522.

1050 Huson D.H., Bryant D. 2006. Application of Phylogenetic Networks in Evolutionary Studies.
1051 Molecular Biology and Evolution. 23:254–267.

1052 Jackson C., McLay T., Schmidt‐Lebuhn A.N. 2023. hybpiper‐nf and paragone‐nf:
1053 Containerization and additional options for target capture assembly and paralog
1054 resolution. Appl Plant Sci. 11:e11532.

1055 Johnson M.G., Gardner E.M., Liu Y., Medina R., Goffinet B., Shaw A.J., Zerega N.J.C.,
1056 Wickett N.J. 2016. HybPiper: Extracting coding sequence and introns for
1057 phylogenetics from high‐throughput sequencing reads using target enrichment.
1058 Applications in Plant Sciences. 4:1600016.

1059 Johnson M.G., Pokorny L., Dodsworth S., Botigué L.R., Cowan R.S., Devault A., Eiserhardt
1060 W.L., Epitawalage N., Forest F., Kim J.T., Leebens-Mack J.H., Leitch I.J., Maurin O.,
1061 Soltis D.E., Soltis P.S., Wong G.K., Baker W.J., Wickett N.J. 2019. A Universal
1062 Probe Set for Targeted Sequencing of 353 Nuclear Genes from Any Flowering Plant
1063 Designed Using k-Medoids Clustering. Systematic Biology. 68:594–606.

1064 Kalyaanamoorthy S., Minh B.Q., Wong T.K.F., von Haeseler A., Jermiin L.S. 2017.
1065 ModelFinder: fast model selection for accurate phylogenetic estimates. Nat Methods.
1066 14:587–589.

1067 Katoh K., Standley D.M. 2013. MAFFT Multiple Sequence Alignment Software Version 7:
1068 Improvements in Performance and Usability. Molecular Biology and Evolution.
1069 30:772–780.

1070 Keller O., Odronitz F., Stanke M., Kollmar M., Waack S. 2008. Scipio: Using protein
1071 sequences to determine the precise exon/intron structures of genes and their orthologs
1072 in closely related species. BMC Bioinformatics. 9:278.

1073 Kent W.J. 2002. BLAT—The BLAST-Like Alignment Tool. Genome Res. 12:656–664.

1074 Kocyan A., Zhang L.-B., Schaefer H., Renner S.S. 2007. A multi-locus chloroplast phylogeny
1075 for the Cucurbitaceae and its implications for character evolution and classification.
1076 Molecular Phylogenetics and Evolution. 44:553–577.

1077 Li D., Liu C.-M., Luo R., Sadakane K., Lam T.-W. 2015. MEGAHIT: an ultra-fast single-
1078 node solution for large and complex metagenomics assembly via succinct de Bruijn
1079 graph. Bioinformatics. 31:1674–1676.

1080 Li D., Luo R., Liu C.-M., Leung C.-M., Ting H.-F., Sadakane K., Yamashita H., Lam T.-W.
1081 2016. MEGAHIT v1.0: A fast and scalable metagenome assembler driven by
1082 advanced methodologies and community practices. Methods. 102:3–11.

1083 Li H.-T., Luo Y., Gan L., Ma P.-F., Gao L.-M., Yang J.-B., Cai J., Gitzendanner M.A.,
1084 Fritsch P.W., Zhang T., Jin J.-J., Zeng C.-X., Wang H., Yu W.-B., Zhang R., Van Der
1085 Bank M., Olmstead R.G., Hollingsworth P.M., Chase M.W., Soltis D.E., Soltis P.S.,
1086 Yi T.-S., Li D.-Z. 2021. Plastid phylogenomic insights into relationships of all
1087 flowering plant families. BMC Biol. 19:232.

Liu B., Ma Z., Ren C., Hodel R.G.J., Sun M., Liu X., Liu G., Hong D., Zimmer E.A., Wen J. 2021. Capturing single‐copy nuclear genes, organellar genomes, and nuclear ribosomal DNA from deep genome skimming data for plant phylogenetics: A case study in Vitaceae. J of Sytematics Evolution. 59:1124–1138.

Matasci N., Hung L.-H., Yan Z., Carpenter E.J., Wickett N.J., Mirarab S., Nguyen N., Warnow T., Ayyampalayam S., Barker M., Burleigh J.G., Gitzendanner M.A., Wafula E., Der J.P., dePamphilis C.W., Roure B., Philippe H., Ruhfel B.R., Miles N.W., Graham S.W., Mathews S., Surek B., Melkonian M., Soltis D.E., Soltis P.S., Rothfels C., Pokorny L., Shaw J.A., DeGironimo L., Stevenson D.W., Villarreal J.C., Chen T., Kutchan T.M., Rolf M., Baucom R.S., Deyholos M.K., Samudrala R., Tian Z., Wu X., Sun X., Zhang Y., Wang J., Leebens-Mack J., Wong G.K.-S. 2014. Data access for the 1,000 Plants (1KP) project. GigaSci. 3:17.

McLay T.G.B., Birch J.L., Gunn B.F., Ning W., Tate J.A., Nauheimer L., Joyce E.M., Simpson L., Schmidt‐Lebuhn A.N., Baker W.J., Forest F., Jackson C.J. 2021. New targets acquired: Improving locus recovery from the Angiosperms353 probe set. Appl Plant Sci. 9:aps3.11420.

Minh B.Q., Hahn M.W., Lanfear R. 2020a. New Methods to Calculate Concordance Factors for Phylogenomic Datasets. Molecular Biology and Evolution. 37:2727–2733.

Minh B.Q., Schmidt H.A., Chernomor O., Schrempf D., Woodhams M.D., von Haeseler A., Lanfear R. 2020b. IQ-TREE 2: New Models and Efficient Methods for Phylogenetic Inference in the Genomic Era. Molecular Biology and Evolution. 37:1530–1534.

Morales-Briones D.F., Kadereit G., Tefarikis D.T., Moore M.J., Smith S.A., Brockington S.F., Timoneda A., Yim W.C., Cushman J.C., Yang Y. 2021. Disentangling Sources of Gene Tree Discordance in Phylogenomic Data Sets: Testing Ancient Hybridizations in Amaranthaceae s.l. Systematic Biology. 70:219–235.

Mower J.P., Stefanović S., Hao W., Gummow J.S., Jain K., Ahmed D., Palmer J.D. 2010. Horizontal acquisition of multiple mitochondrial genes from a parasitic plant followed by gene conversion with host mitochondrial genes. BMC Biol. 8:150.

Nachtigall P.G., Kashiwabara A.Y., Durham A.M. 2021. CodAn: predictive models for precise identification of coding regions in eukaryotic transcripts. Briefings in Bioinformatics. 22:bbaa045.

One Thousand Plant Transcriptomes Initiative. 2019. One thousand plant transcriptomes and the phylogenomics of green plants. Nature. 574:679–685.

Price M.N., Dehal P.S., Arkin A.P. 2010. FastTree 2 – Approximately Maximum-Likelihood Trees for Large Alignments. PLoS ONE. 5:e9490.

Puritz J.B., Hollenbeck C.M., Gold J.R. 2014. *dDocent* : a RADseq, variant-calling pipeline designed for population genomics of non-model organisms. PeerJ. 2:e431.

Raza M., Ortiz E.M., Schwung L., Shigita G., Schaefer H. 2023. Resolving the phylogeny of Thladiantha (Cucurbitaceae) with three different target capture pipelines. BMC Ecol Evo. 23:75.

Renner S.S., Barreda V.D., Tellería M.C., Palazzesi L., Schuster T.M. 2020. Early evolution of Coriariaceae (Cucurbitales) in light of a new early Campanian (ca. 82 Mya) pollen record from Antarctica. TAXON. 69:87–99.

Ribeiro C., Oliveira L., Batista R., De Sousa M. 2021. UCEasy: A software package for automating and simplifying the analysis of ultraconserved elements (UCEs). BDJ. 9:e78132.

Rochette N.C., Rivera‐Colón A.G., Catchen J.M. 2019. Stacks 2: Analytical methods for paired‐end sequencing improve RADseq‐based population genomics. Mol Ecol. 28:4737–4754.

Sayyari E., Whitfield J.B., Mirarab S. 2018. DiscoVista: Interpretable visualizations of gene tree discordance. Molecular Phylogenetics and Evolution. 122:110–115.

Schaefer H. 2020. Cucurbit Website. Version 1. Available from www.cucurbit.de.

Schaefer H., Heibl C., Renner S.S. 2009. Gourds afloat: a dated phylogeny reveals an Asian origin of the gourd family (Cucurbitaceae) and numerous oversea dispersal events. Proc. R. Soc. B. 276:843–851.

Schaefer H., Renner S.S. 2011a. Cucurbitaceae. In: Kubitzki K., editor. The Families and Genera of Flowering Plants. X. Flowering Plants: Eudicots. Sapindales, Cucurbitales, Myrtaceae. Springer, Berlin. p. 112–174.

Schaefer H., Renner S.S. 2011b. Phylogenetic relationships in the order Cucurbitales and a new classification of the gourd family (Cucurbitaceae). Taxon. 60:122–138.

de Sena Brandine G., Smith A.D. 2021. Falco: high-speed FastQC emulation for quality control of sequencing data. F1000Res. 8:1874.

Slater G., Birney E. 2005. Automated generation of heuristics for biological sequence comparison. BMC Bioinformatics. 6:31.

Soltis D.E., Soltis P.S., Morgan D.R., Swensen S.M., Mullin B.C., Dowd J.M., Martin P.G. 1995. Chloroplast gene sequence data suggest a single origin of the predisposition for symbiotic nitrogen fixation in angiosperms. Proc. Natl. Acad. Sci. U.S.A. 92:2647–2651.

Steenwyk J.L., Buida T.J., Li Y., Shen X.-X., Rokas A. 2020. ClipKIT: A multiple sequence alignment trimming software for accurate phylogenomic inference. PLoS Biol. 18:e3001007.

Steinegger M., Söding J. 2018. Clustering huge protein sequence sets in linear time. Nat Commun. 9:2542.

Stevens P.F. 2001. Angiosperm Phylogeny Website. Version 14, July 2017 [and more or less continuously updated since]. Available from http://www.mobot.org/MOBOT/research/APweb/.

Stull G.W., Pham K.K., Soltis P.S., Soltis D.E. 2023. Deep reticulation: the long legacy of hybridization in vascular plant evolution. The Plant Journal.

Tange O. 2021. GNU Parallel 20220422 ('Буча'). Zenodo.

The Angiosperm Phylogeny Group. 2016. An update of the Angiosperm Phylogeny Group classification for the orders and families of flowering plants: APG IV. Bot. J. Linn. Soc. 181:1–20.

Yan Z., Smith M.L., Du P., Hahn M.W., Nakhleh L. 2022. Species Tree Inference Methods Intended to Deal with Incomplete Lineage Sorting Are Robust to the Presence of Paralogs. Systematic Biology. 71:367–381.

Yang Y., Smith S.A. 2014. Orthology Inference in Nonmodel Organisms Using Transcriptomes and Low-Coverage Genomes: Improving Accuracy and Matrix Occupancy for Phylogenomics. Molecular Biology and Evolution. 31:3081–3092.

Zhang C., Mirarab S. 2022. ASTRAL-Pro 2: ultrafast species tree reconstruction from multi-copy gene family trees. Bioinformatics. 38:4949–4950.

Zhang C., Scornavacca C., Molloy E.K., Mirarab S. 2020. ASTRAL-Pro: Quartet-Based Species-Tree Inference despite Paralogy. Molecular Biology and Evolution. 37:3292–3307.

Zhang L.-B., Simmons M.P., Kocyan A., Renner S.S. 2006. Phylogeny of the Cucurbitales based on DNA sequences of nine loci from three genomes: Implications for morphological and sexual system evolution. Molecular Phylogenetics and Evolution. 39:305–322.

Zhang L.-B., Simmons M.P., Renner S.S. 2007. A phylogeny of Anisophylleaceae based on six nuclear and plastid loci: Ancient disjunctions and recent dispersal between South America, Africa, and Asia. Molecular Phylogenetics and Evolution. 44:1057–1067.

Zuntini A.R., Carruthers T., Maurin O., Bailey P.C., Leempoel K., Brewer G.E., Epitawalage N., Françoso E., Gallego-Paramo B., McGinnie C., Negrão R., Roy S.R., Simpson L., Toledo Romero E., Barber V.M.A., Botigué L., Clarkson J.J., Cowan R.S., Dodsworth S., Johnson M.G., Kim J.T., Pokorny L., Wickett N.J., Antar G.M., DeBolt L., Gutierrez K., Hendriks K.P., Hoewener A., Hu A.-Q., Joyce E.M., Kikuchi I.A.B.S., Larridon I., Larson D.A., De Lírio E.J., Liu J.-X., Malakasi P., Przelomska N.A.S., Shah T., Viruel J., Allnutt T.R., Ameka G.K., Andrew R.L., Appelhans M.S., Arista M., Ariza M.J., Arroyo J., Arthan W., Bachelier J.B., Bailey C.D., Barnes H.F., Barrett M.D., Barrett R.L., Bayer R.J., Bayly M.J., Biffin E., Biggs N., Birch J.L., Bogarín D., Borosova R., Bowles A.M.C., Boyce P.C., Bramley G.L.C., Briggs M., Broadhurst L., Brown G.K., Bruhl J.J., Bruneau A., Buerki S., Burns E., Byrne M., Cable S., Calladine A., Callmander M.W., Cano Á., Cantrill D.J., Cardinal-McTeague W.M., Carlsen M.M., Carruthers A.J.A., De Castro Mateo A., Chase M.W., Chatrou L.W., Cheek M., Chen S., Christenhusz M.J.M., Christin P.-A., Clements M.A., Coffey S.C., Conran J.G., Cornejo X., Couvreur T.L.P., Cowie I.D., Csiba L., Darbyshire I., Davidse G., Davies N.M.J., Davis A.P., Van Dijk K., Downie S.R., Duretto M.F., Duvall M.R., Edwards S.L., Eggli U., Erkens R.H.J., Escudero M., De La Estrella M., Fabriani F., Fay M.F., Ferreira P.D.L., Ficinski S.Z., Fowler R.M., Frisby S., Fu L., Fulcher T., Galbany-Casals M., Gardner E.M., German D.A., Giaretta A., Gibernau M., Gillespie L.J., González C.C., Goyder D.J., Graham S.W., Grall A., Green L., Gunn B.F., Gutiérrez D.G., Hackel J., Haevermans T., Haigh A., Hall J.C., Hall T., Harrison M.J., Hatt S.A., Hidalgo O., Hodkinson T.R., Holmes

G.D., Hopkins H.C.F., Jackson C.J., James S.A., Jobson R.W., Kadereit G., Kahandawala I.M., Kainulainen K., Kato M., Kellogg E.A., King G.J., Klejevskaja B., Klitgaard B.B., Klopper R.R., Knapp S., Koch M.A., Leebens-Mack J.H., Lens F., Leon C.J., Léveillé-Bourret É., Lewis G.P., Li D.-Z., Li L., Liede-Schumann S., Livshultz T., Lorence D., Lu M., Lu-Irving P., Luber J., Lucas E.J., Luján M., Lum M., Macfarlane T.D., Magdalena C., Mansano V.F., Masters L.E., Mayo S.J., McColl K., McDonnell A.J., McDougall A.E., McLay T.G.B., McPherson H., Meneses R.I., Merckx V.S.F.T., Michelangeli F.A., Mitchell J.D., Monro A.K., Moore M.J., Mueller T.L., Mummenhoff K., Munzinger J., Muriel P., Murphy D.J., Nargar K., Nauheimer L., Nge F.J., Nyffeler R., Orejuela A., Ortiz E.M., Palazzesi L., Peixoto A.L., Pell S.K., Pellicer J., Penneys D.S., Perez-Escobar O.A., Persson C., Pignal M., Pillon Y., Pirani J.R., Plunkett G.M., Powell R.F., Prance G.T., Puglisi C., Qin M., Rabeler R.K., Rees P.E.J., Renner M., Roalson E.H., Rodda M., Rogers Z.S., Rokni S., Rutishauser R., De Salas M.F., Schaefer H., Schley R.J., Schmidt-Lebuhn A., Shapcott A., Al-Shehbaz I., Shepherd K.A., Simmons M.P., Simões A.O., Simões A.R.G., Siros M., Smidt E.C., Smith J.F., Snow N., Soltis D.E., Soltis P.S., Soreng R.J., Sothers C.A., Starr J.R., Stevens P.F., Straub S.C.K., Struwe L., Taylor J.M., Telford I.R.H., Thornhill A.H., Tooth I., Trias-Blasi A., Udovicic F., Utteridge T.M.A., Del Valle J.C., Verboom G.A., Vonow H.P., Vorontsova M.S., De Vos J.M., Al-Wattar N., Waycott M., Welker C.A.D., White A.J., Wieringa J.J., Williamson L.T., Wilson T.C., Wong S.Y., Woods L.A., Woods R., Worboys S., Xanthos M., Yang Y., Zhang Y.-X., Zhou M.-Y., Zmarzty S., Zuloaga F.O., Antonelli A., Bellot S., Crayn D.M., Grace O.M., Kersey P.J., Leitch I.J., Sauquet H., Smith S.A., Eiserhardt W.L., Forest F., Baker W.J. 2024. Phylogenomics and the rise of the angiosperms. Nature. 629:843–850.

1236 **Supplementary Material**

1237 SUPPLEMENTARY METHOD. Decontamination process for target capture sample *Lemurosicyos*
1238 *variegata*.

1239

1240 TABLE S1. List of samples sequenced for this study.

1241 TABLE S2. List of samples with public data used in this study.

1242 TABLE S3. Per-sample comparison of running time, number of loci recovered, total CDS
1243 length recovered, and average number of paralogs per recovered locus among CAPTUS,
1244 HYBPIPER-BLASTX, and HYBPIPER-DIAMOND.

1245 TABLE S4. Summary statistics per sample at each analysis step.

1246 TABLE S5. Samples lacking sufficient chloroplast data for phylogenetic estimation or with
1247 chloroplast contamination.

1248 TABLE S6. Mitochondrial affinities in the Apodanthaceae. The number of copies found is
1249 indicated next to the letter abbreviations for the species. A=*Apodanthes casearіae*,
1250 Pa=*Pilostyles aethiopica*, Pt=*Pilostyles thurberi*.

1251 FIGURE S1. The CAPTUS output formats, **a)** outputs available when a protein extraction (`NUC`,
1252 `PTD`, `MIT`) is performed, **b)** outputs available when a miscellaneous DNA extraction (`DNA`,
1253 `CLR`) is performed.

1254 FIGURE S2. Total aligned ungapped length per sample using different nuclear reference targets
1255 sets, **a)** Angiosperms353, **b)** Mega353, **c)** RNA5435.

1256 FIGURE S3. Coalescent species trees estimated with ASTRAL-PRO using gene trees estimated
1257 by IQ-TREE on alignments derived from different reference targets sets (RNA5435,
1258 Angiosperms353, Mega353) and paralog filtering strategies (`unfiltered`, `informed`,
1259 `naive`).

1260 FIGURE S4. Species tree estimated by IQ-TREE on the concatenated alignments derived from
1261 the Plastome38 reference targets set.

1262 FIGURE S5. DISCOVISTA analyses of relative quartet frequencies imposed on the coalescent
1263 ASTRAL-PRO topology shown in Fig. S3a using sets of gene trees derived from the different
1264 reference target sets (RNA5435, Angiosperms353, Mega353) calculated by different
1265 programs (IQ-TREE, FASTTREE) and filtered for paralogs (`informed`, `naive`).
1266 FIGURE S6. Phylogenetic network estimate for the Cucurbitales calculated with SPLITSTREE
1267 using the Neighbor Net algorithm on the concatenated alignment of the Angiosperms353
1268 alignments which were filtered using the informed filter of CAPTUS.
1269 FIGURE S7. Relationship between sequencing depth and locus recovery for each datatype.
1270 FIGURE S8. Distribution of sequencing depth of loci recovered by CAPTUS. Loci are classified
1271 according to whether they were recovered only by CAPTUS, or also by HYBPIPER-BLASTX or
1272 HYBPIPER-DIAMOND. Vertical dashed lines indicate the median value for each series.
1273 FIGURE S9. Comparison of paralog sensitivity between pipelines for each data type. Statistical
1274 testing was performed using the Wilcoxon rank-sum test with Bonferroni correction: * $p <$
1275 0.05, ** $p < 0.01$.
1276 FIGURE S10. Coalescent species trees of 80 samples selected for the benchmarking, estimated
1277 from CDS alignments filtered or unfiltered for paralogs. Vertical bar along each tree color-
1278 codes the different tribes/families in the Cucurbitales. Red diamonds indicate nodes with a
1279 local posterior probability below 0.9. Tribes inferred as polyphyletic groups in the HYBPIPER
1280 trees are indicated by their names and positions.
1281
1282 APPENDIX S1. Plastome segments used as reference targets provided as a file in FASTA
1283 format `Plastome38.fasta`
1284 APPENDIX S2. Newly found nuclear putative homologs used as reference targets provided as a
1285 file in FASTA format `RNA5435.fasta`
1286 APPENDIX S3. Estimated species trees in NEWICK format.
1287 APPENDIX S4. Alignments and trees of the mitochondrial regions in NEXUS format.

1288 APPENDIX S5. Benchmarking data: Trimmed gene alignments in FASTA format and their
1289 estimated gene and species trees in NEWICK format.
1290 APPENDIX S6. Reference targets sets used in the decontamination of *Lemurosicyos variegata*
1291 (Supplementary Method).